

Supplementary Material for

Multi-Pyridine Decorated Fe(II) and Ru(II) complexes by Pd(0)-Catalysed Cross Couplings: New Building Blocks for Metallosupramolecular Assemblies

Jiajia Yang,^a Jack K. Clegg,^c Qibai Jiang,^a Xiaoming Liu,^d Hong Yan,^a Wei Zhong^d and Jonathon E. Beves,^{a,b,*}

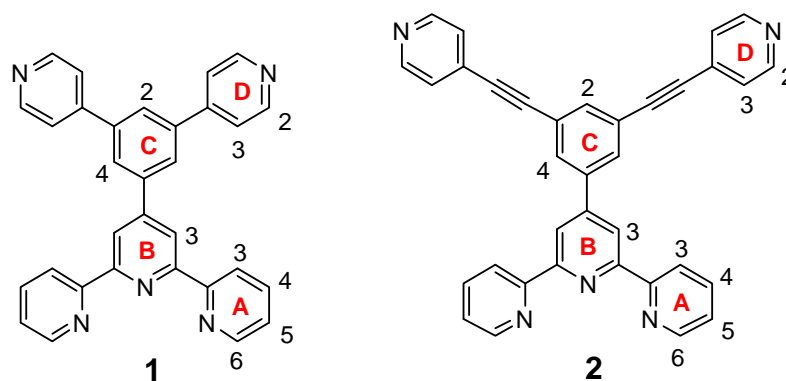
S1. General Experimental Methods	3
S2. Synthesis of Ligands 1 and 2	4
2.1.1 Synthesis of 4'-(3,5-di(pyridin-4-yl)phenyl)-2,2':6',2''-terpyridine (1)	4
2.1.2 Synthesis of 4'-(3,5-bis(pyridin-4-ylethynyl)phenyl)-2,2':6',2''-terpyridine (2)	7
S3. Synthesis and Characterisation of Fe(II) complexes	9
3.1.1 Synthesis of [Fe(1) ₂](PF ₆) ₂	9
3.1.2 Synthesis of [Fe(2) ₂](PF ₆) ₂	12
S4. Synthesis of Ru(II) complexes	15
4.1.1 Synthesis of Ru(4'-(3,5-dibromophenyl)-2,2':6':2''-terpyridine) ₂ (PF ₆) ₂ Ru(5) ₂ (PF ₆) ₂	15
4.1.2 Synthesis and Characterisation of [Ru(1) ₂](PF ₆) ₂	19
4.1.3 Synthesis and Characterisation of [Ru(2) ₂](PF ₆) ₂	23
S5. Synthesis of <i>N</i> -alkylated Ru(II) derivatives	26
5.1.1 Synthesis and Characterisation of [Ru(3a) ₂](PF ₆) ₆	26
5.1.2 Synthesis and Characterisation of [Ru(4a) ₂](PF ₆) ₆	30
5.1.3 Synthesis and Characterisation of [Ru(3b) ₂](PF ₆) ₆	33
5.1.4 Synthesis and Characterisation of [Ru(4b) ₂](PF ₆) ₆	37
S6. Summary of Absorption Data	41
S7. Electrochemical Data	42
7.1.1 Cyclic Voltammograms of [Fe(1) ₂](PF ₆) ₂ and [Ru(1) ₂](PF ₆) ₂	42
7.1.2 Cyclic Voltammograms of [Fe(2) ₂](PF ₆) ₂ and [Ru(2) ₂](PF ₆) ₂	43
7.1.3 Cyclic Voltammograms of <i>N</i> -Me complexes [Ru(3a) ₂](PF ₆) ₆ and [Ru(4a) ₂](PF ₆) ₆	44
7.1.4 Cyclic Voltammograms of <i>N</i> -C ₁₂ H ₂₅ complexes [Ru(3b) ₂](PF ₆) ₆ and [Ru(4b) ₂](PF ₆) ₆	45
7.1.5 Electrochemical data for [Fe(4'-phenyl-(2,2':6',6''-terpyridine) ₂](PF ₆) ₂	46
7.1.6 Differential Pulse Voltammetry (DPV) for [Ru(1) ₂](PF ₆) ₂ , [Ru(3a) ₂](PF ₆) ₆ and [Ru(3b) ₂](PF ₆) ₆	47
7.1.7 Summary of electrochemical data	48
S8. X-Ray diffraction experimental	49
8.1.1 General	49
8.1.2 Data for structure [Ru(1) ₂]·2PF ₆ ·8.25H ₂ O	49
8.1.3 Data for structure [Fe(1) ₂]·2PF ₆ ·6MeNO ₂ ·12.5H ₂ O	50
8.1.4 Data for structure 3 [Ru(1) ₂]·5PF ₆ ·NO ₃	51
8.1.5 Data for [Ru(2) ₂](PF ₆) ₂	52

S9. Host-Guest Interactions	53
9.1.1 Pillar[n]arenes	53
9.1.2 Metal-ion coordination by [Ru(3a) ₂](PF ₆) ₂	54
9.1.3 Metal-ion coordination by [Ru(3b) ₂](PF ₆) ₂	56
9.1.4 Association constant determinations	58
S10. Additional References	61

S1. General Experimental Methods

^1H and $^{13}\text{C}\{^1\text{H}\}$ NMR spectra were recorded on a Bruker AM-500 spectrometer (500MHz); the numbering scheme adopted for the ligands is shown in Scheme 1. The chemical shifts for the ^1H and $^{13}\text{C}\{^1\text{H}\}$ NMR spectra are referenced to residual solvent peaks with respect to TMS $\delta = 0$ ppm. Electrospray (ESI) mass spectra were recorded using a Finnigan MAT LSQ7000 mass spectrometer and high-resolution ESI-MS on a Agilent 6540Q-TOF liquid chromatography/mass spectrometry (LC/MS) system. UV-VIS spectra were recorded on Shimadzu UV-2550 spectrophotometers. X-ray diffraction data were collected on a Bruker SMART APEX CCD II single-crystal diffractometer. Melting points (uncorrected) were determined using a X-4 melting point apparatus from Beijing Kaifu (China). Electrochemical measurements were conducted in freshly distilled acetonitrile with 0.1M TBAPF₆ electrolyte solution using a CHI600D instrument made by Chinese Shanghai Chenhua instrument co., with a glassy carbon working electrode, platinum counter electrode, Ag wire as a pseudo-reference and calibrated with internal ferrocene added at the end of the experiment. All column chromatography separations were carried out on silica gel 60 (200-300 mesh, Huanghai Chemical Reagent Company). Compounds 4'-(3,5-dibromophenyl)-2,2':6',2''-terpyridine¹, 4-ethynylpyridine², 4-pyridineboronic acid pinacol ester³ and Ru(DMSO)₄Cl₂⁴ were prepared by literature methods.

S2. Synthesis of Ligands 1 and 2



Scheme 1 Structures of ligands **1** and **2**, and atom number scheme for NMR spectroscopic data.

2.1.1 Synthesis of 4'-(3,5-di(pyridin-4-yl)phenyl)-2,2':6',2''-terpyridine (**1**)

4'-(3,5-Dibromophenyl)-2,2':6',2''-terpyridine (200 mg, 0.43 mmol), 4-pyridineboronic acid pinacol ester (0.26 g, 1.3 mmol, 3 equiv.) and CsCO₃ (0.83 g, 4.3 mol, 10 equiv.) were dissolved in degassed DMF (10 mL). The solution was bubbled with argon for 10 min. Pd(PPh₃)₄ (100 mg, 0.09 mmol., 20 %) were added quickly and bubbled with argon for another 10 min. The solution was stirred at 80 °C for 12h. The solvent was removed to give a pale yellow sludge which was dissolved in 10% MeOH in DCM (30 mL) and absorbed on SiO₂. Column chromatography (SiO₂, DCM: MeOH: NEt₃ 100:2:0.001) gave the title compound as a white solid (170 mg, 0.55 mmol, 85%). ¹H NMR (500 MHz, CDCl₃) δ 8.81 (s, 2H, H^{B3}), 8.79 – 8.73 (m, 6H, H^{A6+D2}), 8.72 (d, *J* = 8.0 Hz, 2H, H^{A3}), 8.17 (s, 2H, H^{C4}), 7.95 – 7.88 (m, 3H, H^{A4+C2}), 7.67 (d, *J* = 4.5 Hz, 4H, H^{D3}), 7.42 – 7.36 (m, 2H, H^{A5}). ¹³C{¹H} NMR (125 MHz, CDCl₃) δ 156.4 (C^{B2}), 156.1 (C^{A2}), 150.6 (C^{D2}), 149.5 (C^{C5}), 149.3 (C^{A6}), 147.7 (C^{C1}), 141.0 (C^{B4}), 140.3 (C^{D4}), 137.2 (C^{A4}), 126.8 (C^{C4}), 126.4 (C^{C2}), 124.3 (C^{A5}), 122.1 (C^{D3}), 121.6 (C^{A3}), 119.1 (C^{B3}). LR-ESI-MS *m/z* found 464.42 (LH⁺), requires 464.19 *m/z*. HR-ESI-MS found 464.1873 (LH⁺), requires: 464.1870. m.p. 260-262 °C

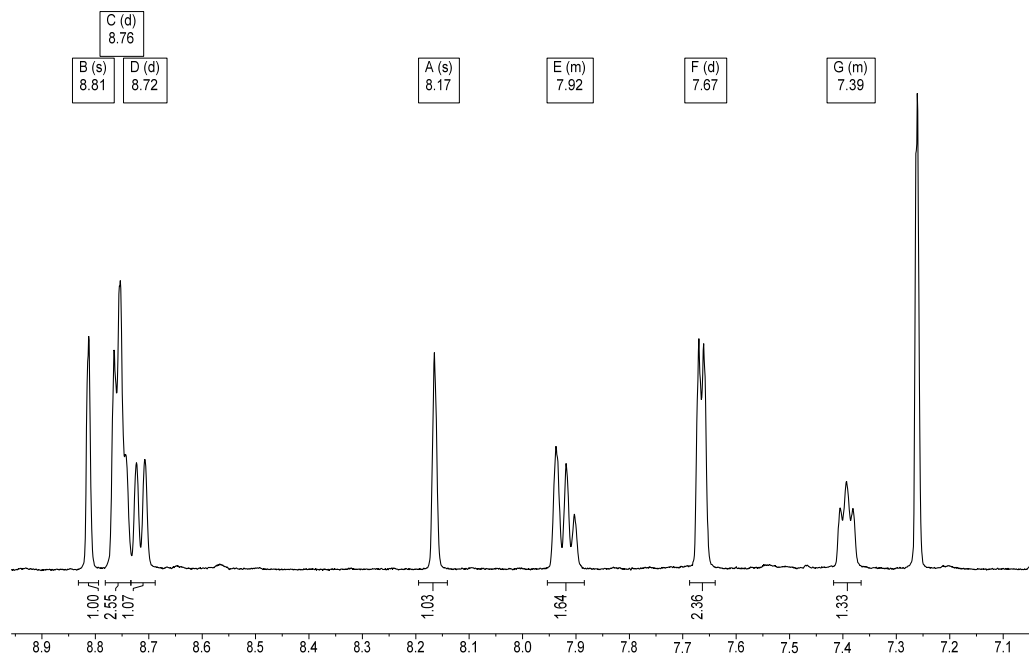


Figure S1 $^1\text{H-NMR}$ (CDCl_3 , 500 MHz) of compound **1**

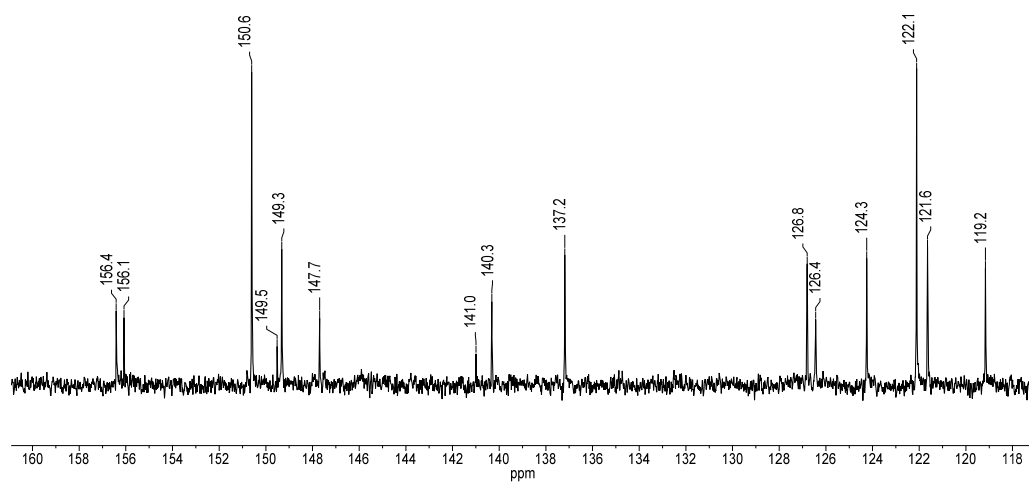


Figure S2 $^{13}\text{C}\{^1\text{H}\}$ -NMR (CDCl_3 , 125 MHz) of compound **1**

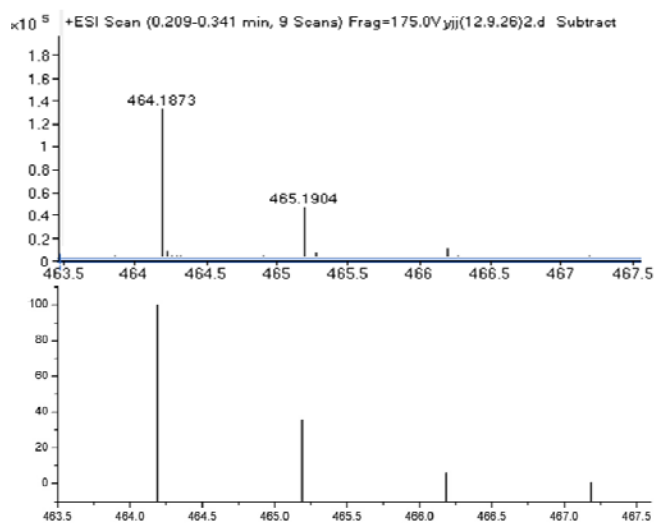


Figure S3 High resolution ESI-MS peak of $[1H]^+$ with calculated spectrum below.

2.1.2 Synthesis of 4'-(3,5-bis(pyridin-4-ylethynyl)phenyl)-2,2':6',2''-terpyridine (2)

4'-(3,5-Dibromophenyl)-2,2':6',2''-terpyridine (100 mg, 0.21 mmol) and 4-ethynylpyridine (62 mg, 0.6 mmol, 3 equiv.) was dissolved in degassed (three freeze-pump-thaw cycles) THF (15 mL) and freshly distilled diethylamine (5 mL), the solution was bubbled with argon for 10 min. Pd(PPh₃)₄ (50 mg, 0.04 mmol, 20 %) were added quickly and bubbled with argon for another 10 min. The solution was stirred at 65 °C for 24h. The solvent was removed to give a yellow sludge which was dissolved in ethyl acetate (30 mL) and absorbed on SiO₂. Column chromatography (SiO₂, petroleum ether: ethyl acetate: NEt₃ 5: 2: 0.001) gave the title compound as a white solid (90 mg, 0.18 mmol, 84%). ¹H NMR (500 MHz, CDCl₃) δ 8.76 (m, 4H, H^{A6+B3}), 8.71 (d, *J* = 7.9 Hz, 2H, H^{A3}), 8.65 (dd, *J* = 4.5, 1.5 Hz, 4H, H^{D2}), 8.11 (d, *J* = 1.4 Hz, 2H, H^{C4}), 7.91 (td, *J* = 7.8, 1.7 Hz, 2H, H^{A4}), 7.83 (t, *J* = 1.3 Hz, 1H, H^{C2}), 7.44 (dd, *J* = 4.5, 1.5 Hz, 4H, H^{D3}), 7.39 (ddd, *J* = 7.4, 4.6, 1.0 Hz, 2H, H^{A5}). ¹³C{¹H} NMR (101 MHz, CDCl₃) δ 156.4 (C^{B2}), 156.0 (C^{A2}), 150.1 (C^{D2}), 149.3 (C^{A6}), 148.4 (C^{C5}), 139.8 (C^{B4}), 137.2 (C^{A4}), 135.3 (C^{C2}), 131.3 (C^{C4}), 131.0 (C^{D4}), 125.7 (C^{D3}), 124.3 (C^{A5}), 123.7 (C^{C1}), 121.6 (C^{A3}), 118.8 (C^{B3}), 92.4 (C^{C-alkyne}), 88.1 (C^{D-alkyne}). LR-ESI-MS *m/z* found 511.5 (LH⁺), requires 512.2 *m/z*. HR-ESI-MS found 512.1882, requires 512.1870. m.p. 304-306°C

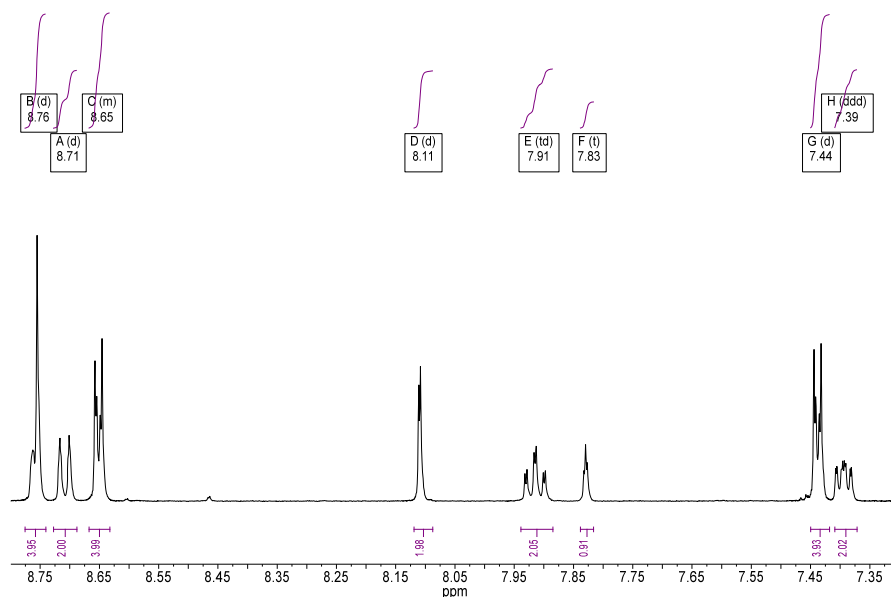


Figure S4 ¹H-NMR (CDCl₃, 500 MHz) of compound 2.

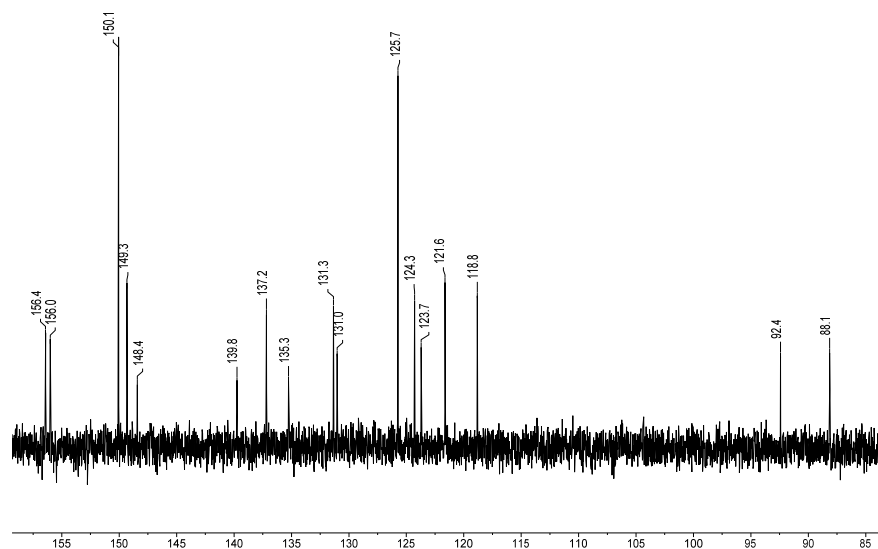


Figure S5 $^{13}\text{C}\{^1\text{H}\}$ -NMR (CDCl_3 , 101 MHz) of compound **2**.

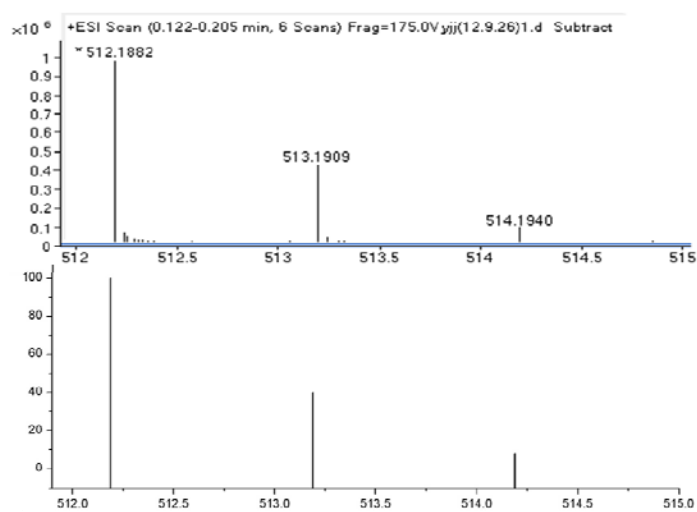
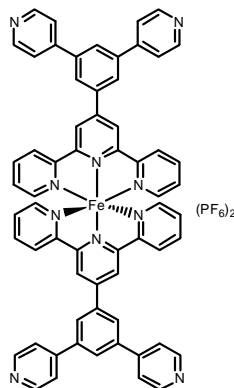


Figure S6 High-resolution ESI-MS spectrum of peak of $[\mathbf{2H}]^+$ with calculated spectrum below.

S3. Synthesis and Characterisation of Fe(II) complexes

3.1.1 Synthesis of $[\text{Fe}(\mathbf{1})_2](\text{PF}_6)_2$



Ligand **1** (22 mg, 0.04 mmol) and $\text{FeCl}_2 \cdot 4\text{H}_2\text{O}$ (4.1 mg, 0.02 mmol) were dissolved in EtOH (20 mL) and the reaction mixture was stirred at room temperature for 1 h. Excess ethanolic NH_4PF_6 was added and the resulting purple precipitate was collected on Celite and washed well with water (3×10 mL), EtOH (2×2 mL) and Et_2O (20 mL). The residue was dissolved in MeCN and the solvent removed to give $[\text{Fe}(\mathbf{1})_2][\text{PF}_6]_2$ as a purple powder (25 mg, 0.019 mmol, 90%). ^1H NMR (500 MHz, CD_3CN) δ 9.38 (s, 2H, $\text{H}^{\text{B}3}$), 8.82 (d, $J = 5.6$ Hz, 4H, $\text{H}^{\text{D}2}$), 8.72 (m, 4H, $\text{H}^{\text{C}4+\text{A}3}$), 8.39 (s, 1H, $\text{H}^{\text{C}2}$), 8.01 (d, $J = 5.7$ Hz, 4H, $\text{H}^{\text{D}3}$), 7.95 (t, $J = 7.6$ Hz, 2H, $\text{H}^{\text{A}4}$), 7.23 (d, $J = 5.5$ Hz, 2H, $\text{H}^{\text{A}6}$), 7.13 (t, $J = 6.5$ Hz, 2H, $\text{H}^{\text{A}5}$). $^{13}\text{C}\{^1\text{H}\}$ NMR (125 MHz, CD_3CN) δ 161.4 ($\text{C}^{\text{B}2}$), 158.9 ($\text{C}^{\text{A}2}$), 154.0 ($\text{C}^{\text{A}6}$), 151.5 ($\text{C}^{\text{D}2}$), 150.3 ($\text{C}^{\text{C}5}$), 147.8 ($\text{C}^{\text{C}1}$), 141.4 ($\text{C}^{\text{D}4}$), 139.8 ($\text{C}^{\text{A}4}$), 139.6 ($\text{C}^{\text{B}4}$), 128.8 ($\text{C}^{\text{C}2}$), 128.4 ($\text{C}^{\text{A}5}$), 128.1 ($\text{C}^{\text{C}4}$), 125.0 ($\text{C}^{\text{A}3}$), 123.0 ($\text{C}^{\text{B}3+\text{D}3}$). LR-ESI-MS m/z 491.58 $[\text{M}-2\text{PF}_6]^{2+}$ requires 491.15, 1127.67 $[\text{M}-\text{PF}_6]^+$ requires 1127.26; HR-MS m/z 491.1492 $[\text{M}-2\text{PF}_6]^{2+}$ requires 491.1495.

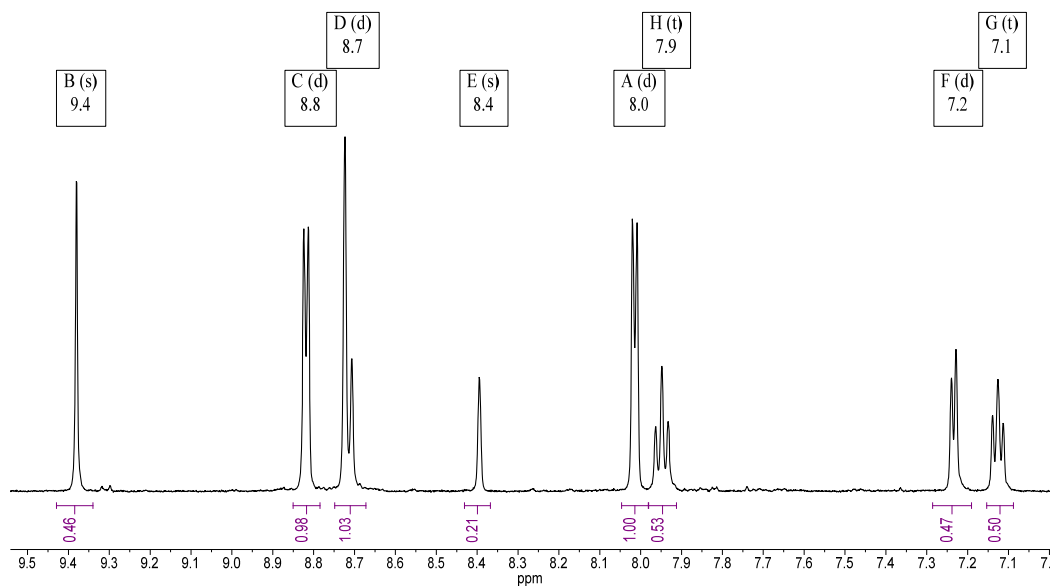


Figure S7 $^1\text{H-NMR}$ (CD_3CN , 500 MHz) of compound $[\text{Fe}(\mathbf{1})_2](\text{PF}_6)_2$ with added NEt_3

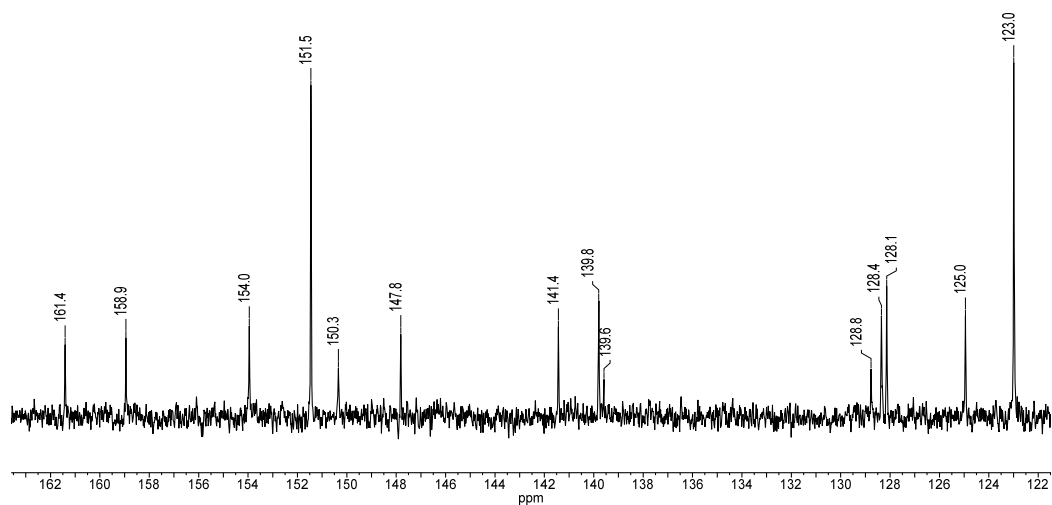


Figure S8 $^{13}\text{C}\{^1\text{H}\}$ -NMR (CD_3CN , 125 MHz) of compound $[\text{Fe}(\mathbf{1})_2](\text{PF}_6)_2$ with added NEt_3

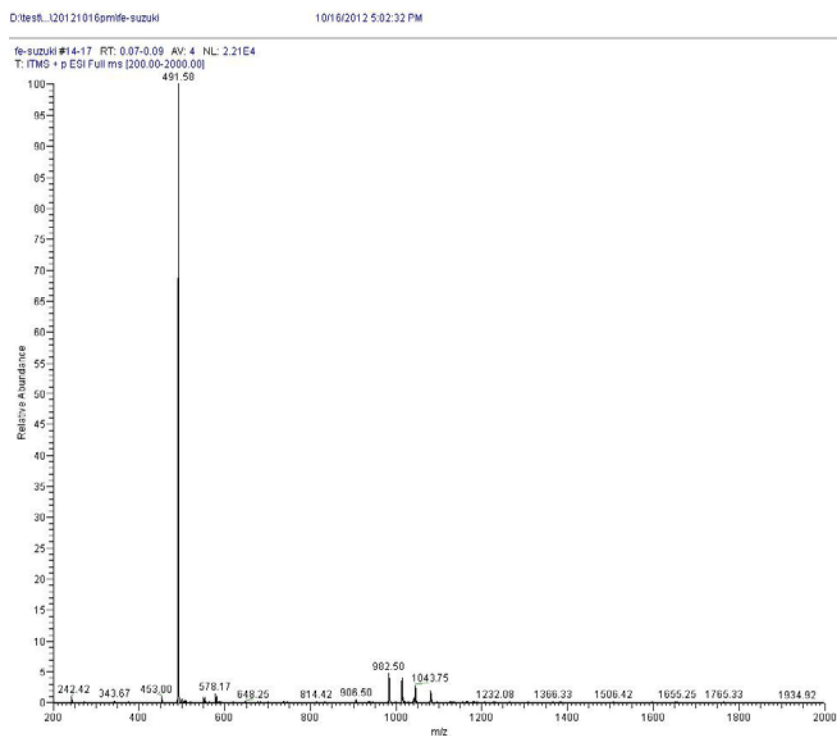


Figure S9 Low resolution ESI-MS spectrum of compound $[\text{Fe}(\mathbf{1})_2][\text{PF}_6]_2$

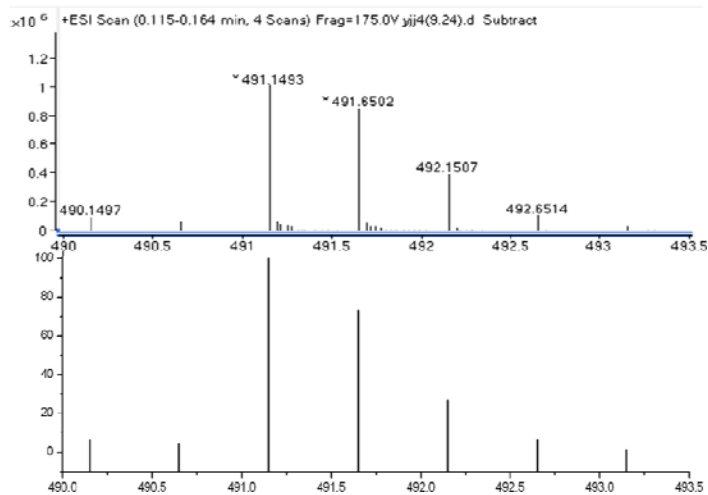
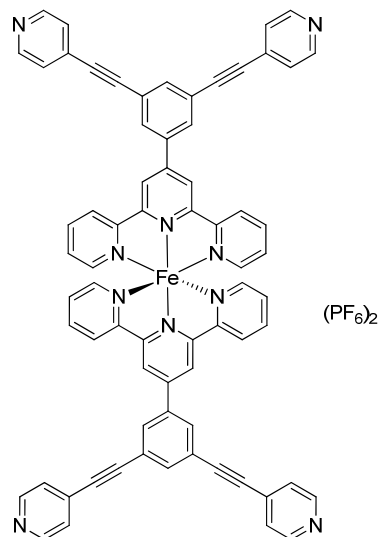


Figure S10 High resolution ESI-MS of peak $[\text{Fe}(\mathbf{1})_2]^{2+}$ with calculated spectrum below.

3.1.2 Synthesis of $[\text{Fe}(\mathbf{2})_2](\text{PF}_6)_2$



Ligand **2** (20 mg, 0.04 mmol) and $\text{FeCl}_2 \cdot 4\text{H}_2\text{O}$ (4.1 mg, 0.02 mmol) were dissolved in EtOH (20 mL) and the reaction mixture was stirred at room temperature for 1 h. Excess ethanolic NH_4PF_6 was added and the resulting purple precipitate was collected on Celite and washed well with water (3×10 mL), EtOH (2×2 mL) and Et_2O (20 mL). The residue was dissolved in MeCN and the solvent removed to give $[\text{Fe}(\mathbf{2})_2][\text{PF}_6]_2$ as a purple powder (24 mg, 0.019 mmol, 90%). ^1H NMR (500 MHz, CD_3CN) δ 9.26 (s, 2H, $\text{H}^{\text{B}3}$), 8.69 (d, $J = 4.5$ Hz, 4H, $\text{H}^{\text{D}2}$), 8.66 (d, $J = 8.0$ Hz, 2H, $\text{H}^{\text{A}3}$), 8.59 (s, 2H, $\text{H}^{\text{C}4}$), 8.12 (s, 1H, $\text{H}^{\text{C}2}$), 7.95 (t, $J = 7.7$ Hz, 2H, $\text{H}^{\text{A}4}$), 7.58 (d, $J = 4.5$ Hz, 4H, $\text{H}^{\text{D}3}$), 7.21 (d, $J = 5.5$ Hz, 2H, $\text{H}^{\text{A}6}$), 7.12 (t, $J = 6.5$ Hz, 2H, $\text{H}^{\text{A}5}$). $^{13}\text{C}\{^1\text{H}\}$ NMR (125 MHz, CD_3CN) δ 161.5 ($\text{C}^{\text{B}2}$), 158.8 ($\text{C}^{\text{A}2}$), 154.0 ($\text{C}^{\text{A}6}$), 151.1 ($\text{C}^{\text{D}2}$), 149.1 ($\text{C}^{\text{C}5}$), 139.8 ($\text{C}^{\text{A}4}$), 139.0 ($\text{C}^{\text{B}4}$), 137.0 ($\text{C}^{\text{C}2}$), 132.7 ($\text{C}^{\text{C}4}$), 131.2 ($\text{C}^{\text{D}4}$), 128.4 ($\text{C}^{\text{A}5}$), 126.4 ($\text{C}^{\text{D}3}$), 125.1 ($\text{C}^{\text{C}1}$), 124.9 ($\text{C}^{\text{A}3}$), 122.6 ($\text{C}^{\text{B}3}$), 92.3 ($\text{C}^{\text{C-alkyne}}$), 89.2 ($\text{C}^{\text{D-alkyne}}$). LR-ESI-MS m/z found 539.67 $[\text{M}-2\text{PF}_6]^{2+}$, requires 539.15 m/z , $[\text{M}-\text{PF}_6]^+$ 1223.68 requires 1223.26; HR-ESI-MS found 539.1488 $[\text{M}-2\text{PF}_6]^{2+}$ requires 539.1495.

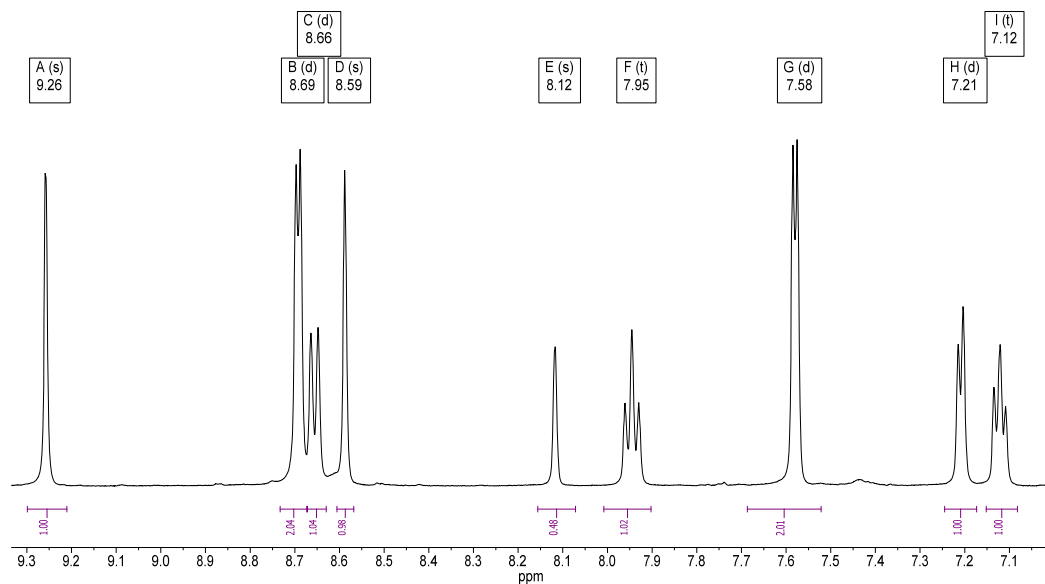


Figure S11 $^1\text{H-NMR}$ (CD_3CN , 500 MHz) of compound $[\text{Fe}(\mathbf{2})_2][\text{PF}_6]_2$ with added NEt_3

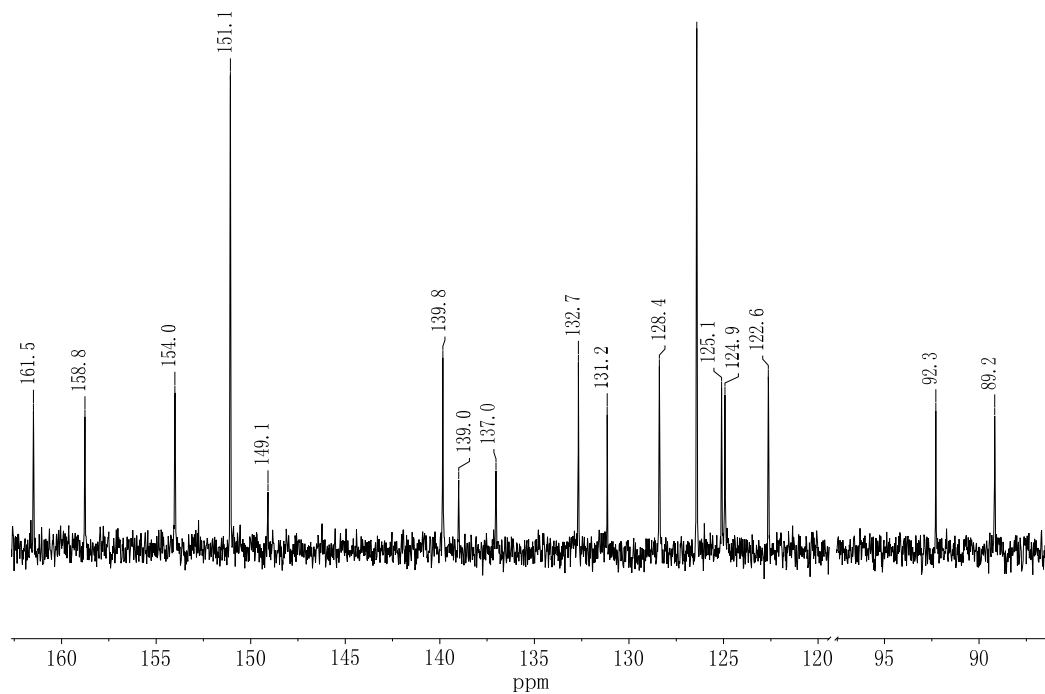


Figure S12 $^{13}\text{C}\{^1\text{H}\}$ -NMR (CD_3CN , 125 MHz) of compound $[\text{Fe}(\mathbf{2})_2][\text{PF}_6]_2$ with added NEt_3 .

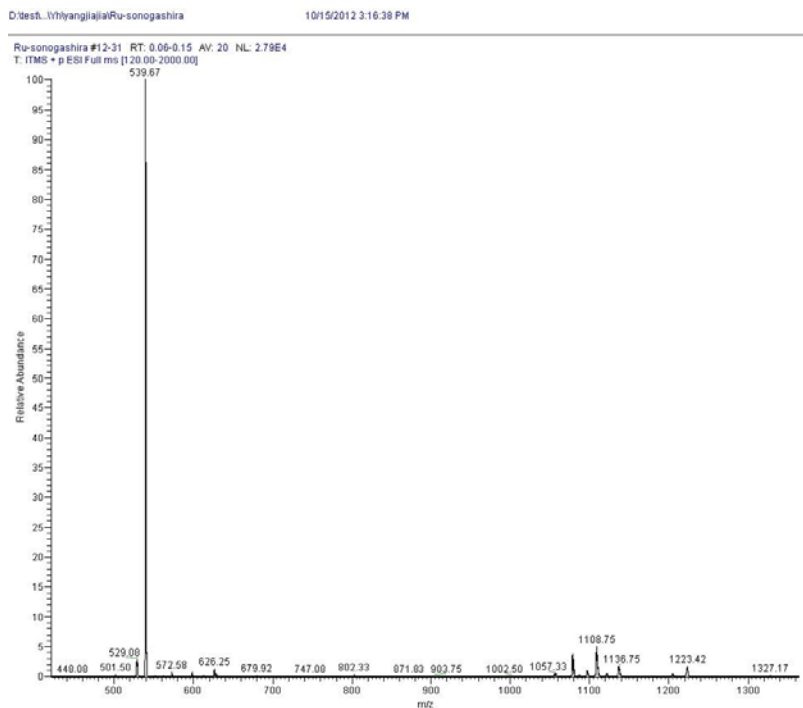


Figure S13 Low resolution ESI-MS spectrum of compound $[\text{Fe}(\mathbf{2})_2][\text{PF}_6]_2$.

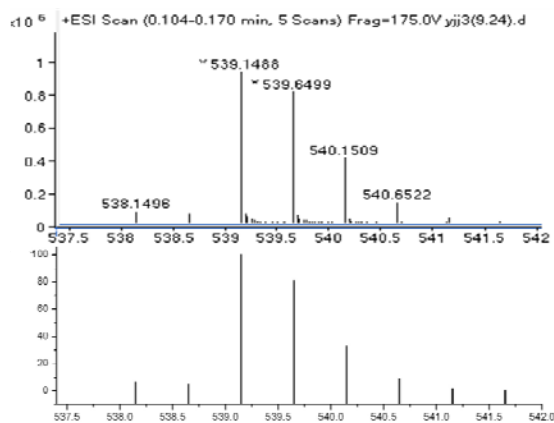


Figure S14 High resolution ESI-MS peak of $[\text{Fe}(\mathbf{2})_2]^{2+}$ with calculated spectrum below.

S4. Synthesis of Ru(II) complexes

[Ru(4'-(3,5-dibromophenyl)-2,2':6':2''-terpyridine)₂](PF₆)₂ is a known complex,⁵ although no previous synthetic or spectroscopic data appears to be published. Here it was prepared using standard procedures.⁶

4.1.1 Synthesis of Ru(4'-(3,5-dibromophenyl)-2,2':6':2''-terpyridine)₂(PF₆)₂ Ru(5)₂(PF₆)₂

4'-(3,5-dibromophenyl)-2,2':6',2''-terpyridine (**5**) (0.40 g, 0.85 mmol) and [Ru(DMSO)₄Cl₂]₂ (0.19 g, 0.39 mmol) were suspended in ethane-1,2-diol (30 mL) and heated in a microwave (800 W, 140 degrees, 10 min). The deep red solution was cooled to room temperature and poured into excess aqueous NH₄PF₆ (100 mL). The resulting red precipitate was collected on Celite and washed well with water (3 × 100 mL), EtOH (2 × 10 mL), CHCl₃ (3 × 50 mL) and Et₂O (20 mL). The remaining residue was dissolved in MeCN and the solvent removed to give [Ru(**5**)₂][PF₆]₂ as a deep red powder (0.51 g, 0.38 mmol, 97%). This was purified by column chromatography (SiO₂, MeCN:H₂O: saturated aqueous KNO₃ 14 : 1 : 1). The centre of the main red band was collected, excess aqueous NH₄PF₆ was added and the volume reduced to precipitate the hexafluorophosphate salt, which was collected and recrystallised from MeCN/H₂O to give a pure microcrystalline red solid (0.46 g, 0.35 mmol, 90%). ¹H NMR (400 MHz, CD₃CN) δ 9.00 (s, 2H, H^{B3}), 8.66 (d, *J* = 8.1 Hz, 2H, H^{A3}), 8.41 (d, *J* = 1.7 Hz, 2H, H^{C4}), 8.06 (s, 1H, H^{C2}), 7.96 (td, *J* = 7.9, 1.4 Hz, 2H, H^{A4}), 7.41 (d, *J* = 5.6 Hz, 2H, H^{A6}), 7.19 (ddd, *J* = 7.2, 5.6, 1.0 Hz, 2H, H^{A5}). ¹³C{¹H} NMR (101 MHz, CD₃CN) δ 158.8 (C^{A2}), 156.5 (C^{B2}), 153.4 (C^{A6}), 146.0 (C^{C5}), 141.4 (C^{B4}), 139.1 (C^{A4}), 136.1 (C^{C2}), 130.7 (C^{C4}), 128.5 (C^{A5}), 125.6 (C^{A3}), 124.7 (C^{C1}), 122.7 (C^{B3}). LR-ESI-MS *m/z* 518.17 [M-2PF₆]²⁺ requires 517.90, 1180.67 [M-PF₆]⁺ requires 1180.77; HR-MS *m/z* 517.9042 [M-2PF₆]²⁺ requires 517.9014, 1180.7652 [M-PF₆]⁺ requires 1180.7670.

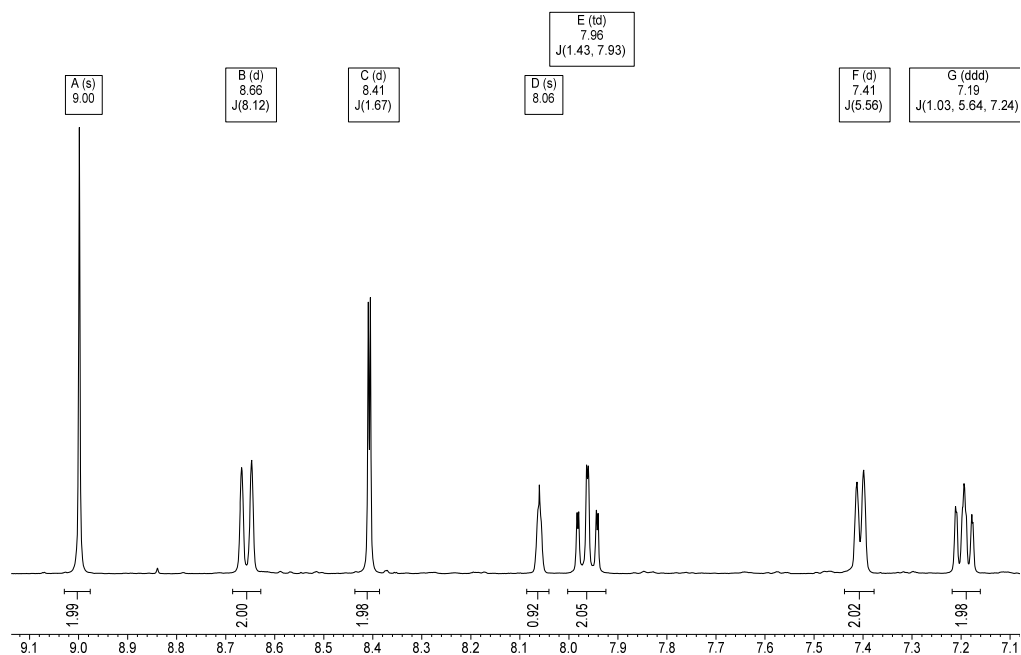


Figure S15 $^1\text{H-NMR}$ (CD_3CN , 400 MHz) of compound $[\text{Ru}(\mathbf{5})_2](\text{PF}_6)_2$

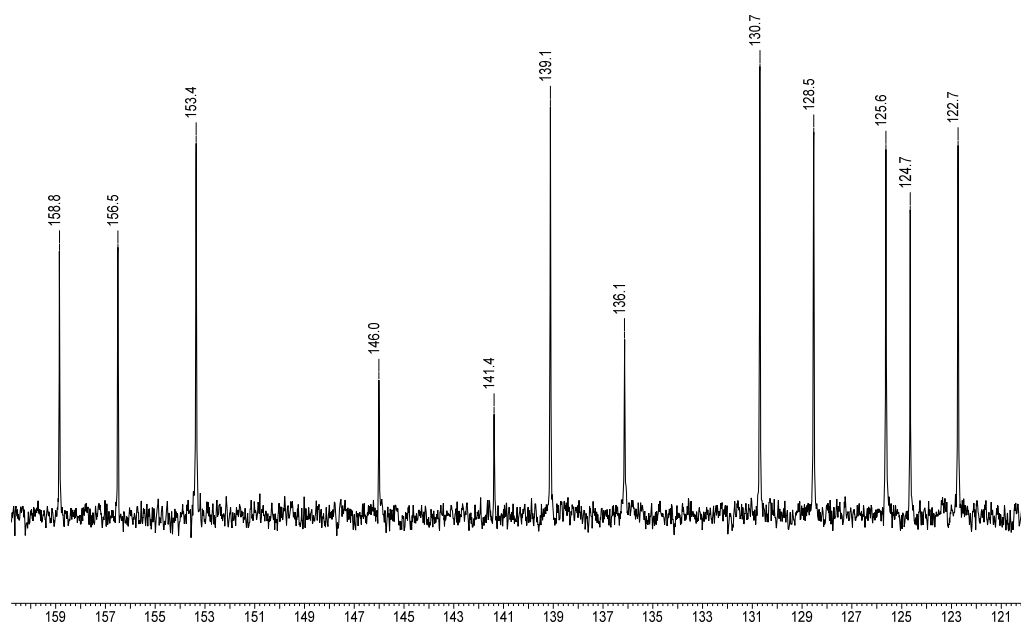


Figure S16 $^{13}\text{C}\{^1\text{H}\}$ -NMR (CD_3CN , 101 MHz) of compound $[\text{Ru}(\mathbf{5})_2](\text{PF}_6)_2$

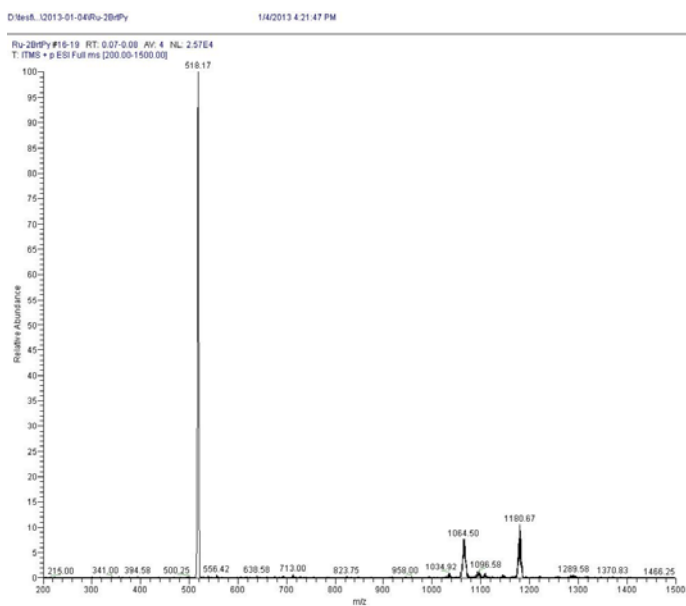


Figure S17 Low resolution ESI-MS spectrum of compound $[\text{Ru}(\mathbf{5})_2](\text{PF}_6)_2$

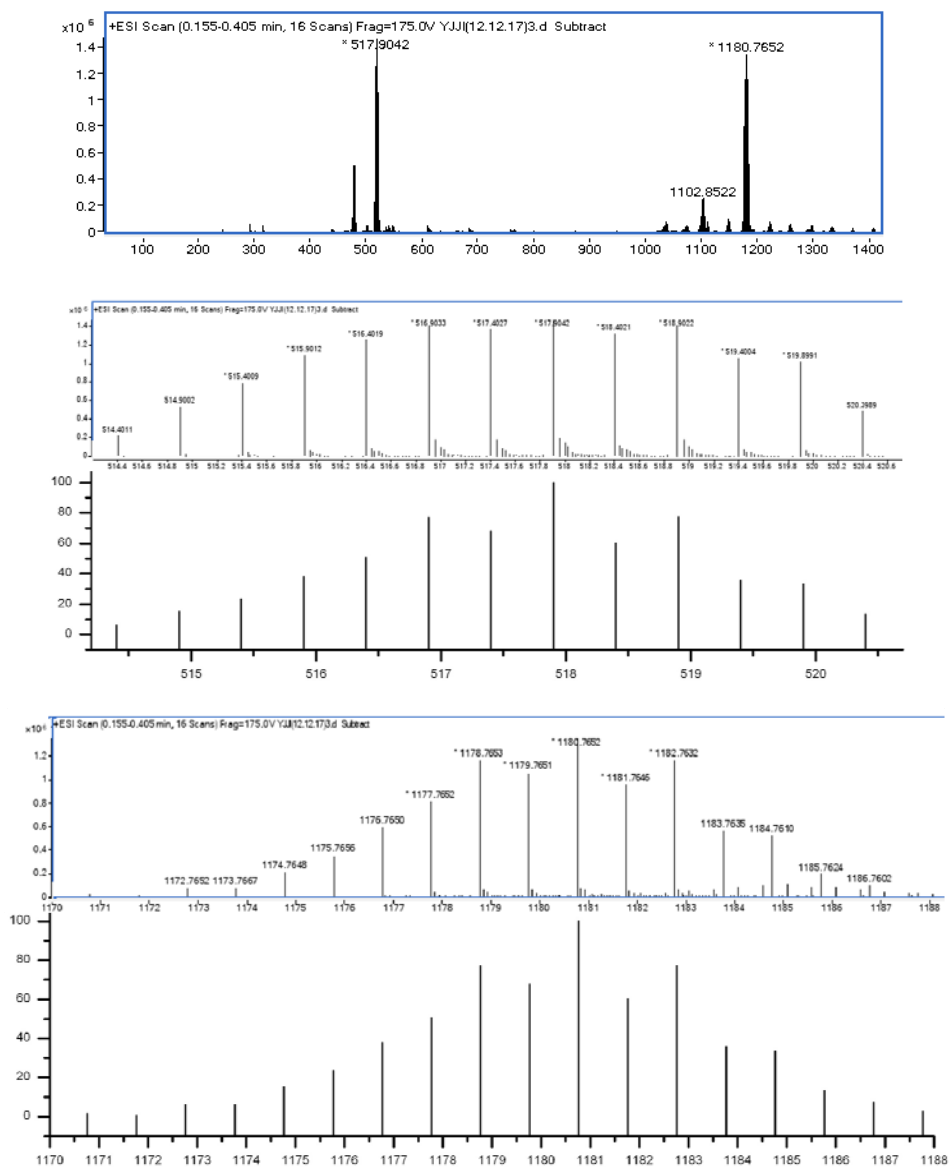
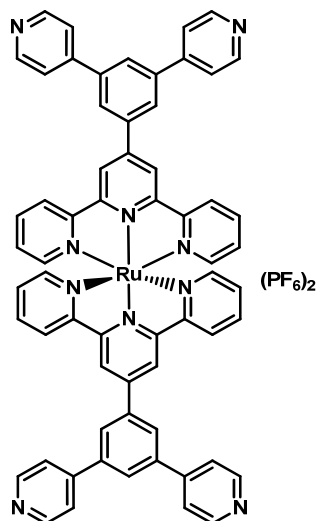


Figure S18 High resolution ESI-MS spectrum of compound $[\text{Ru}(\mathbf{5})_2](\text{PF}_6)_2$, with zooms of $[\text{Ru}(\mathbf{5})_2]^{2+}$ and $[\text{Ru}(\mathbf{5})_2(\text{PF}_6)]^+$ and simulated spectra shown below each.

4.1.2 Synthesis and Characterisation of [Ru(1)₂](PF₆)₂



[Ru(5)₂](PF₆)₂ (0.32g, 0.24 mmol), 4-pyridineboronic acid pinacol ester (0.30 g, 1.45 mmol, 6 equiv.), CsCO₃ (0.93 g, 4.8 mmol) and NH₄PF₆ (0.32 g, 1.9 mol) was dissolved in degassed DMF (20 mL). The solution was bubbled with argon for 10 min. Pd(PPh₃)₄ (60 mg, 0.05 mmol., 20 %) was added quickly and bubbled with argon for another 10 min. The solution was stirred at 80 °C overnight. The solvent was removed and the residue dissolved in 5 mL MeCN, poured into excess aqueous NH₄PF₆ (100 mL). The resulting red precipitate was collected on Celite and washed well with water (3 × 100 mL), EtOH (2 × 10 mL) and Et₂O (20 mL). The remaining residue was dissolved in MeCN. The solvent was removed to give a red powder which was absorbed on SiO₂ and purified by column chromatography (SiO₂, MeCN: H₂O: saturated aqueous KNO₃ 7 : 1 : 1) gave the title compound [Ru(1)₂](PF₆)₂ as a red solid (268 mg, 0.19 mmol, 85%). ¹H NMR (400 MHz, CD₃CN) δ 9.20 (s, 2H, H^{B3}), 8.81 (d, *J* = 4.6, 1.6 Hz, 4H, H^{D2}), 8.74 (d, *J* = 8.2 Hz, 2H, H^{A3}), 8.61 (d, *J* = 1.5 Hz, H^{C4}), 8.35 (t, *J* = 1.5 Hz, H^{C2}), 8.03 – 7.94 (m, 6H, H^{D3+A4}), 7.47 (d, *J* = 4.9 Hz, 2H, H^{A6}), 7.22 (t, *J* = 6.6 Hz, 2H, H^{A5}). ¹³C{¹H} NMR (101 MHz, CD₃CN) δ 159.1 (C^{A2}), 156.5 (C^{B2}), 153.4 (C^{A6}), 151.4 (C^{D2}), 148.2 (C^{C5}), 147.8 (C^{C1}), 141.3 (C^{D4}), 139.7 (C^{B4}), 139.1 (C^{A4}), 128.5 (C^{C2+A5}), 128.0 (C^{C4}), 125.6 (C^{A3}), 123.0 (C^{B3+D3}). LR-ESI-MS *m/z* 514.40 [M-2PF₆]²⁺ requires 514.13, 1173.44 [M-PF₆]⁺ requires 1173.23; HR-MS *m/z* 514.1331 [M-2PF₆]²⁺ requires 514.1335, 1173.2303 [M-PF₆]⁺ requires 1173.2311.

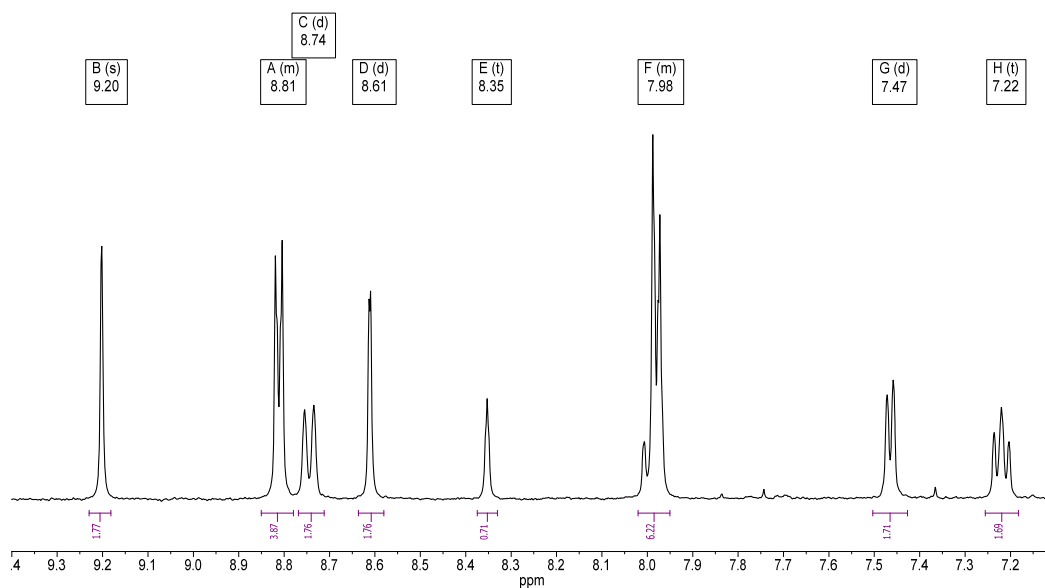


Figure S19 $^1\text{H-NMR}$ (CD_3CN , 400 MHz) of compound $[\text{Ru}(\mathbf{1})_2][\text{PF}_6]_2$ with added NEt_3

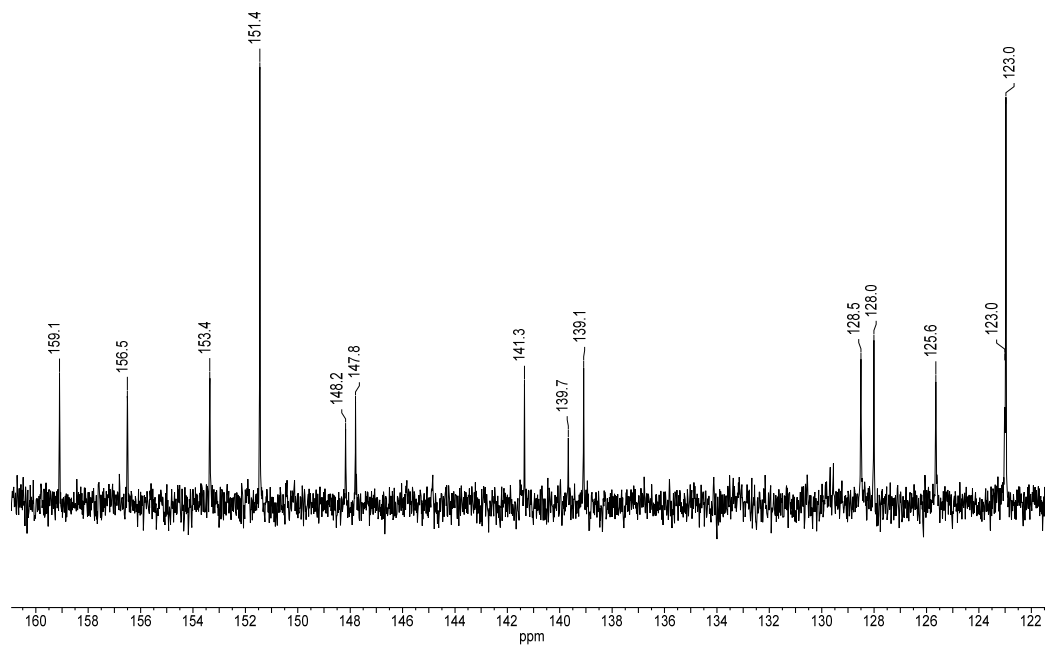


Figure S20 $^{13}\text{C}\{^1\text{H}\}$ -NMR (CD_3CN , 101 MHz) of compound $[\text{Ru}(\mathbf{1})_2][\text{PF}_6]_2$ with added NEt_3

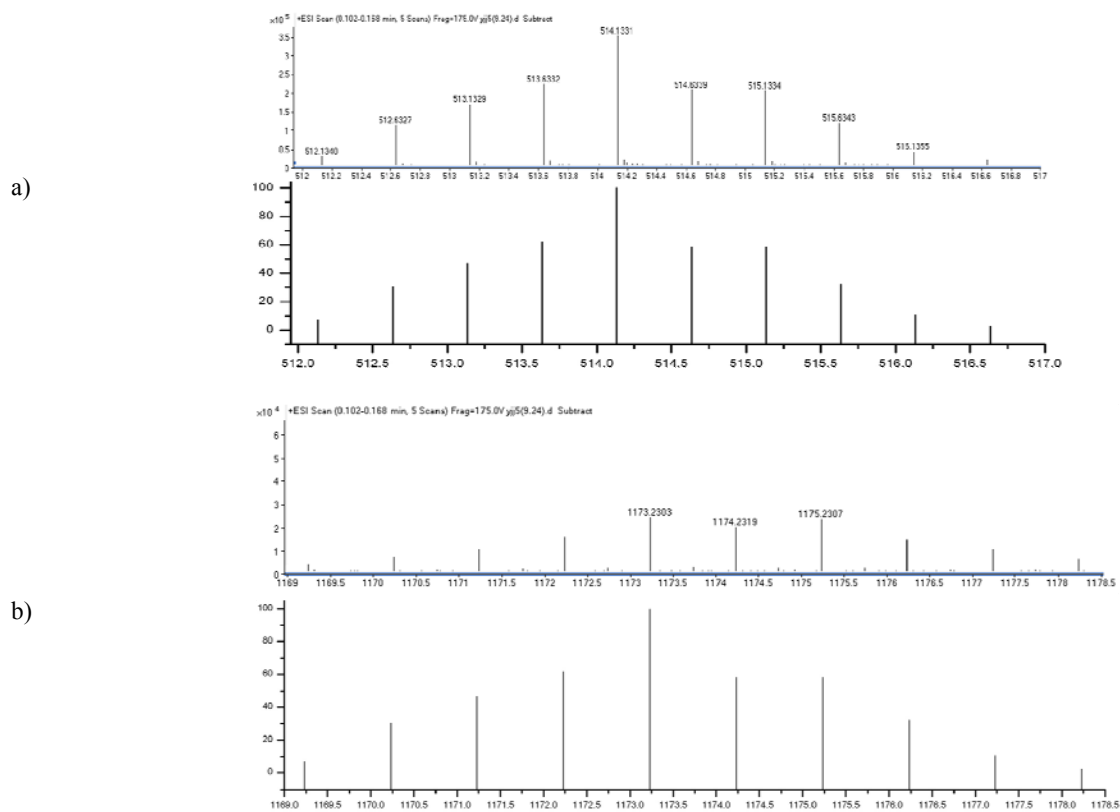
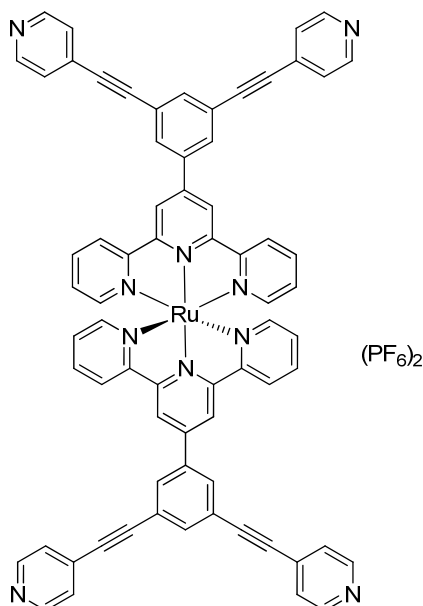


Figure S22 High resolution ESI-MS spectrum of compound $[\text{Ru}(\mathbf{1})_2][\text{PF}_6]_2$. Zoom of a) $[\text{Ru}(\mathbf{1})_2]^{2+}$ and b) $[\text{Ru}(\mathbf{1})_2(\text{PF}_6)]^+$ with calculated spectra below each.

4.1.3 Synthesis and Characterisation of [Ru(2)₂](PF₆)₂



[Ru(5)₂][PF₆]₂ (100 mg, 0.08 mmol), 4-ethynylpyridine (0.62 g, 0.60 mmol, 8 equiv.), CuI (0.8 mg, 0.045 mmol, 60 %) and NH₄PF₆ (20 mg, 0.12 mol) was dissolved in degassed DMF (5 mL) and DME (10 mL). The solution was bubbled with argon for 10 min. Pd(PPh₃)₄ (35 mg, 0.03 mmol, 40 %) was added quickly and bubbled with argon for another 10 min. The solution was stirred at 80 °C overnight. The solvent was removed and the residue dissolved in 5 mL MeCN, poured into excess aqueous NH₄PF₆ (100 mL). The resulting red precipitate was collected on Celite and washed well with water (3 × 100 mL), EtOH (2 × 10 mL) and Et₂O (20 mL). The remaining residue was dissolved in MeCN. The solvent was removed to give a red powder which was absorbed on SiO₂ and purified by column chromatography (SiO₂, MeCN: H₂O: saturated aqueous KNO₃ 10 : 1 : 1) gave the title compound [Ru(2)₂][PF₆]₂ as a red solid (82 mg, 0.058 mmol, 77%). ¹H NMR (400 MHz, CD₃CN) δ 9.09 (s, 2H, H^{B3}), 8.75 – 8.65 (m, 6H, H^{D2+A3}), 8.49 (d, J = 1.1 Hz, 2H, H^{C4}), 8.07 (s, 1H, H^{C2}), 7.98 (t, J = 7.4 Hz, 2H, H^{A4}), 7.56 (dd, J = 4.6, 1.4 Hz, 4H, H^{D3}), 7.45 (d, J = 5.3 Hz, 2H, H^{A6}), 7.22 (t, 2H, H^{A5}). ¹³C{¹H} NMR (101 MHz, CD₃CN) δ 158.9 (C^{A2}), 156.6 (C^{B2}), 153.4 (C^{A6}), 151.1 (C^{D2}), 147.0 (C^{C5}), 139.2 (C^{A4}), 139.1 (C^{B4}), 136.8 (C^{C2}), 132.6 (C^{C4}), 131.2 (C^{D4}), 128.6 (C^{A5}), 126.4 (C^{D3}), 125.6 (C^{A3}), 125.0 (C^{C1}), 122.7 (C^{B3}), 92.3 (C^{C-alkyne}), 89.1 (C^{D-alkyne}). LR-ESI-MS *m/z* 562.34 [M-2PF₆]²⁺ requires 562.13, 1269.34 [M-PF₆]⁺ requires 1269.23; HR-MS *m/z* 562.1340 [M-2PF₆]²⁺ requires 562.1335, 1269.2309 [M-PF₆]⁺ requires 1269.2306.

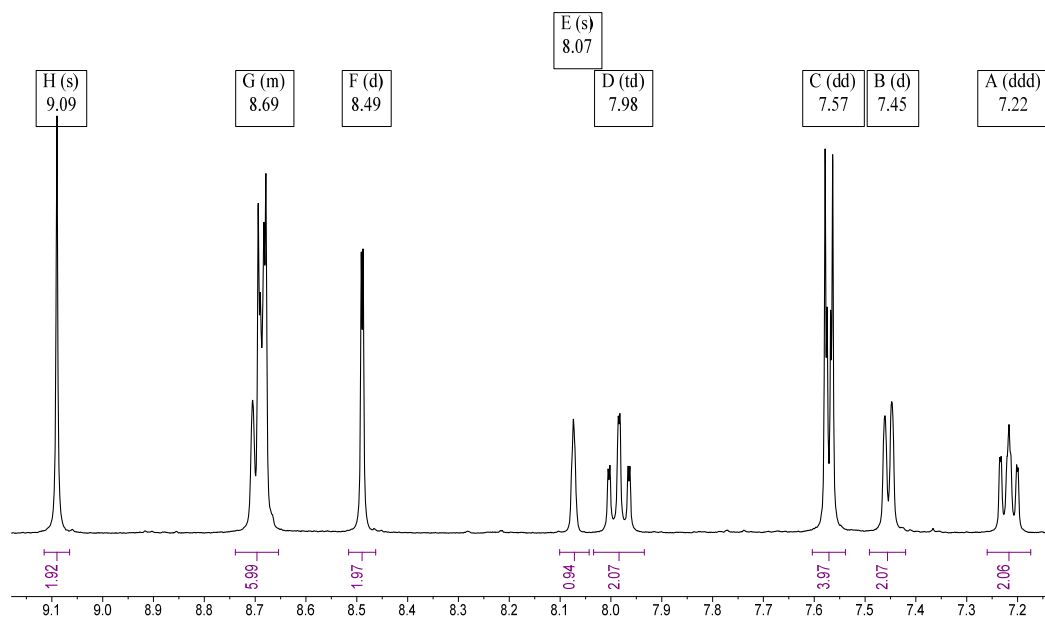


Figure S23 $^1\text{H-NMR}$ (CD_3CN , 400 MHz) of compound $\text{Ru}(\mathbf{2})_2[\text{PF}_6]_2$ with added NEt_3

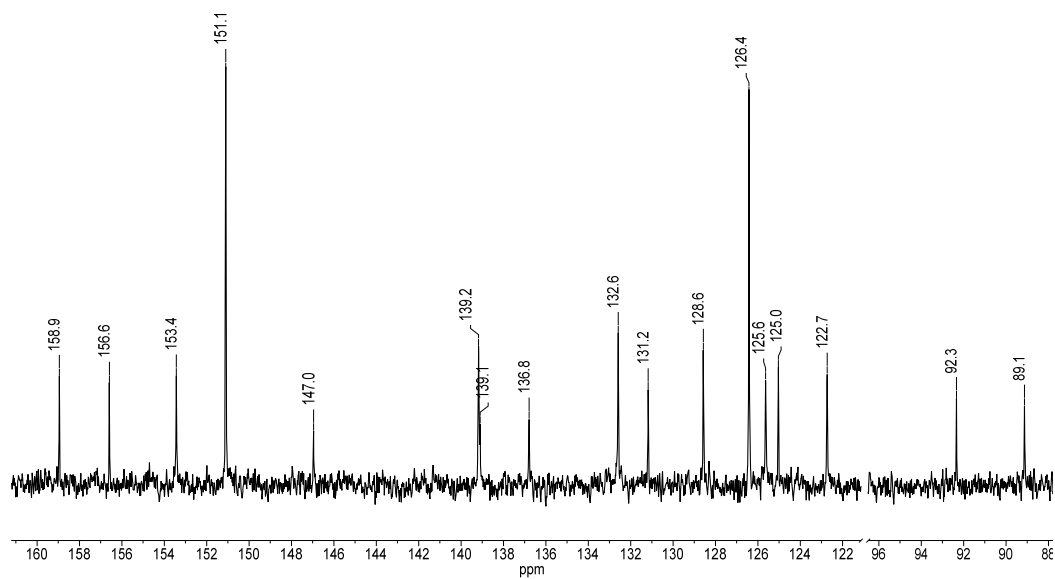


Figure S24 $^{13}\text{C}\{^1\text{H}\}$ -NMR (CD_3CN , 101 MHz) of compound $[\text{Ru}(\mathbf{2})_2](\text{PF}_6)_2$ with added NEt_3

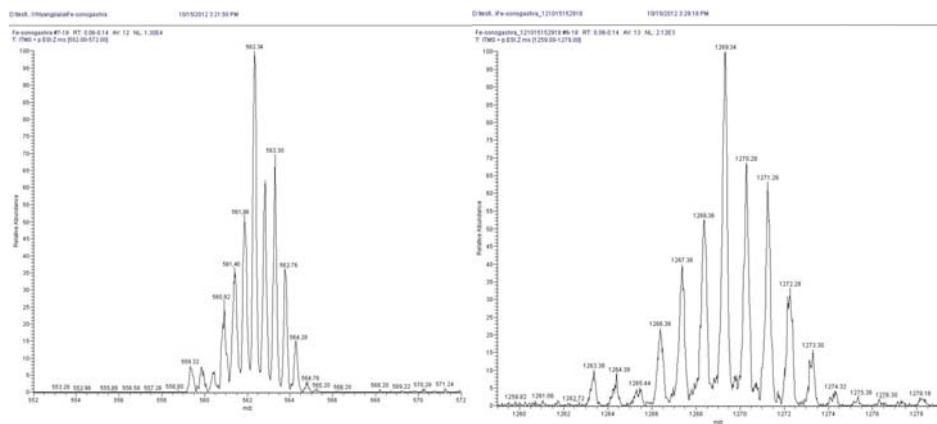


Figure S25 Low resolution ESI-MS spectrum of compound $[\text{Ru}(2)_2][\text{PF}_6]_2$ of signals corresponding to $[\text{Ru}(2)_2]^{2+}$ and $[\text{Ru}(2)_2(\text{PF}_6)]^+$

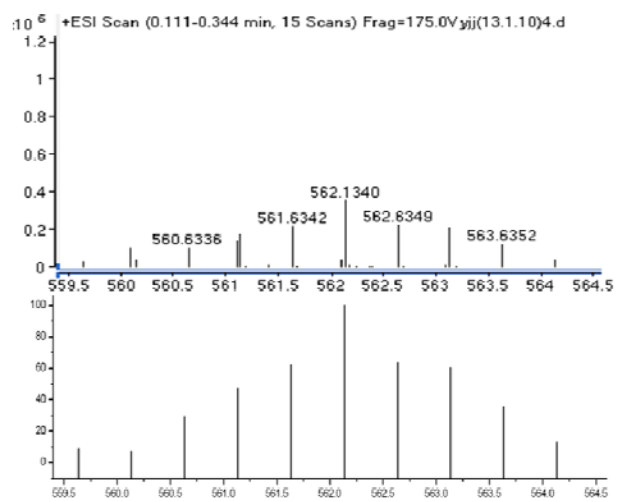
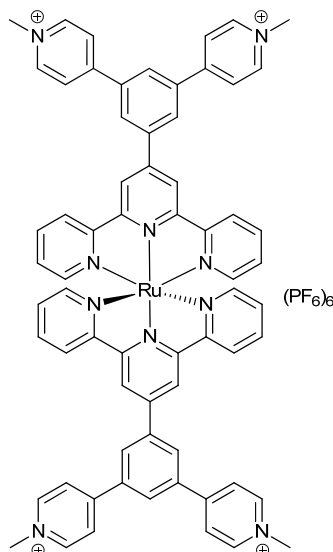


Figure S26 High resolution ESI-MS peak of $[\text{Ru}(2)_2]^{2+}$ with calculated spectra below.

S5. Synthesis of *N*-alkylated Ru(II) derivatives

5.1.1 Synthesis and Characterisation of [Ru(3a)₂](PF₆)₆



[Ru(1)₂](PF₆)₂ (20 mg, 0.015 mmol), NH₄PF₆ (60 mg, 0.2 mmol) and methyl iodide (1 mL, 7 mmol) dissolved in 30 mL MeCN. The solution was refluxed overnight to give a red suspension. Water was added and the volume reduced under reduced pressure. The resulting suspension was collected on Celite, washed well with water, EtOH, DCM and Et₂O. The residue was dissolved in MeCN and the solvent removed to give the title compound [Ru(3a)₂](PF₆)₆ as a red solid (30 mg, 0.015 mmol, 99%). ¹H NMR (500 MHz, CD₃CN) δ 9.24 (s, 2H, H^{B3}), 8.91 (s, 2H, H^{C4}), 8.86 (d, *J* = 6.5 Hz, 4H, H^{D2}), 8.78 (d, *J* = 8.1 Hz, 2H, H^{A3}), 8.66 (d, *J* = 6.5 Hz, 4H, H^{D3}), 8.63 (s, 1H, H^{C2}), 8.01 (t, *J* = 7.8 Hz, 2H, H^{A4}), 7.52 (d, *J* = 5.5 Hz, 2H, H^{A6}), 7.25 (t, *J* = 6.4 Hz, 2H, H^{A5}), 4.42 (s, 6H, H^{Me}). ¹³C {¹H} NMR (126 MHz, CD₃CN) δ 158.9 (C^{A2}), 156.6 (C^{B2}), 155.3 (C^{C1}), 153.4 (C^{A6}), 146.8 (C^{C5}), 146.6 (C^{D2}), 140.8 (C^{B4}), 139.2 (C^{A4}), 137.7 (C^{D4}), 131.3 (C^{C4}), 130.1 (C^{C2}), 128.6 (C^{A5}), 126.7 (C^{D3}), 125.6 (C^{A3}), 123.1 (C^{B3}), 48.8 (Me). LR-ESI-MS found *m/z* 181.75 [M-6PF₆]⁶⁺, requires 181.39; 247.00 [M-5PF₆]⁵⁺ requires 246.66; 344.75 [M-4PF₆]⁴⁺ requires 344.57; 507.58 [M-3PF₆]³⁺ requires 507.75; 834.08 [M-2PF₆]²⁺ requires 834.11. HR-ESI-MS *m/z* found 181.3939 [M-6PF₆]⁶⁺ requires 181.3935; 246.6135 [M-5PF₆]⁵⁺ requires 246.6650; 344.5726 [M-4PF₆]⁴⁺ requires 344.5723; 507.7520 [M-3PF₆]³⁺ requires 507.7511; 834.1093 [M-2PF₆]²⁺ requires 834.1088.

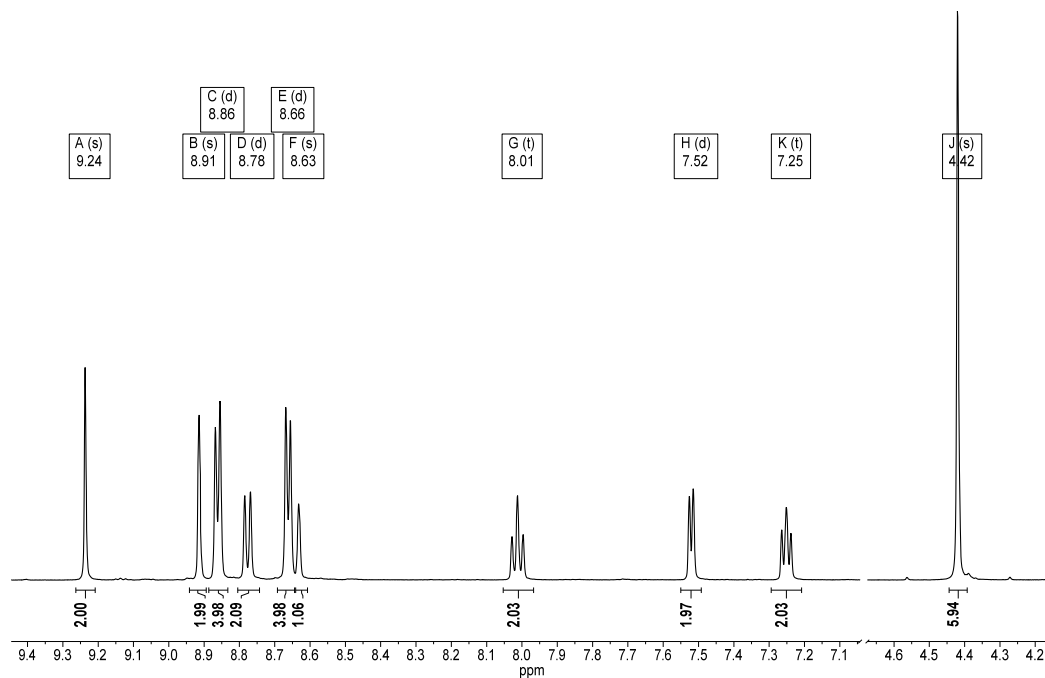


Figure S27 $^1\text{H-NMR}$ (CD_3CN , 500 MHz) of compound $[\text{Ru}(\mathbf{3a})_2][\text{PF}_6]_6$

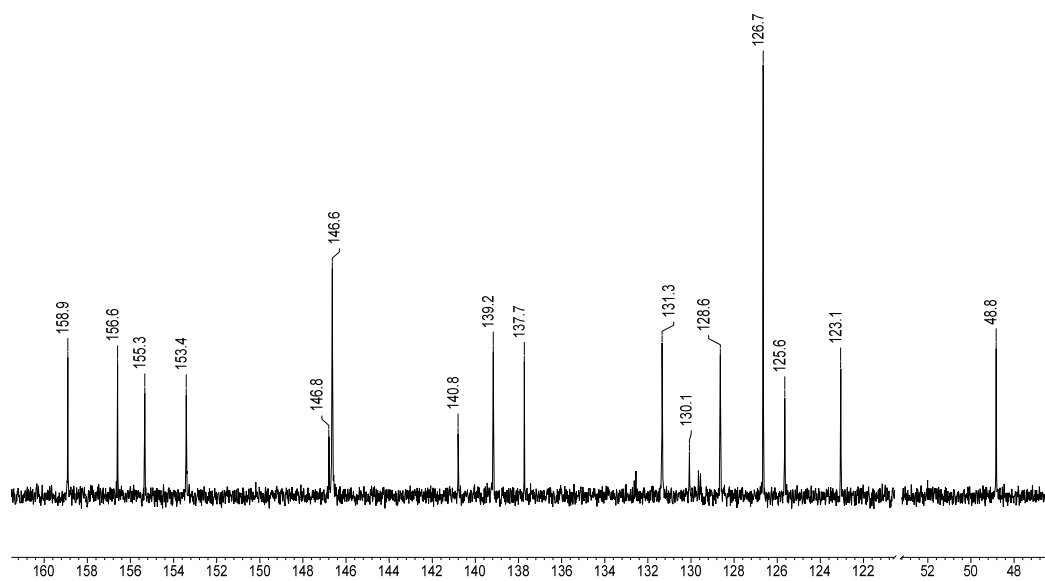


Figure S28 $^{13}\text{C}\{^1\text{H}\}$ -NMR (CD_3CN , 126 MHz) of compound $[\text{Ru}(\mathbf{3a})_2][\text{PF}_6]_6$

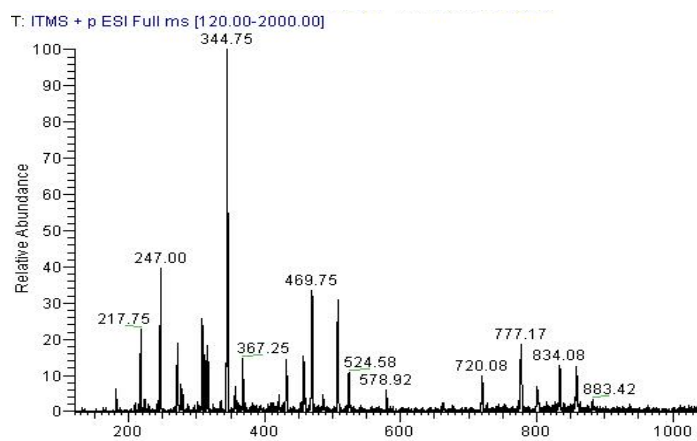


Figure S29 Low resolution ESI-MS spectrum of compound $[\text{Ru}(\mathbf{3a})_2][\text{PF}_6]_6$

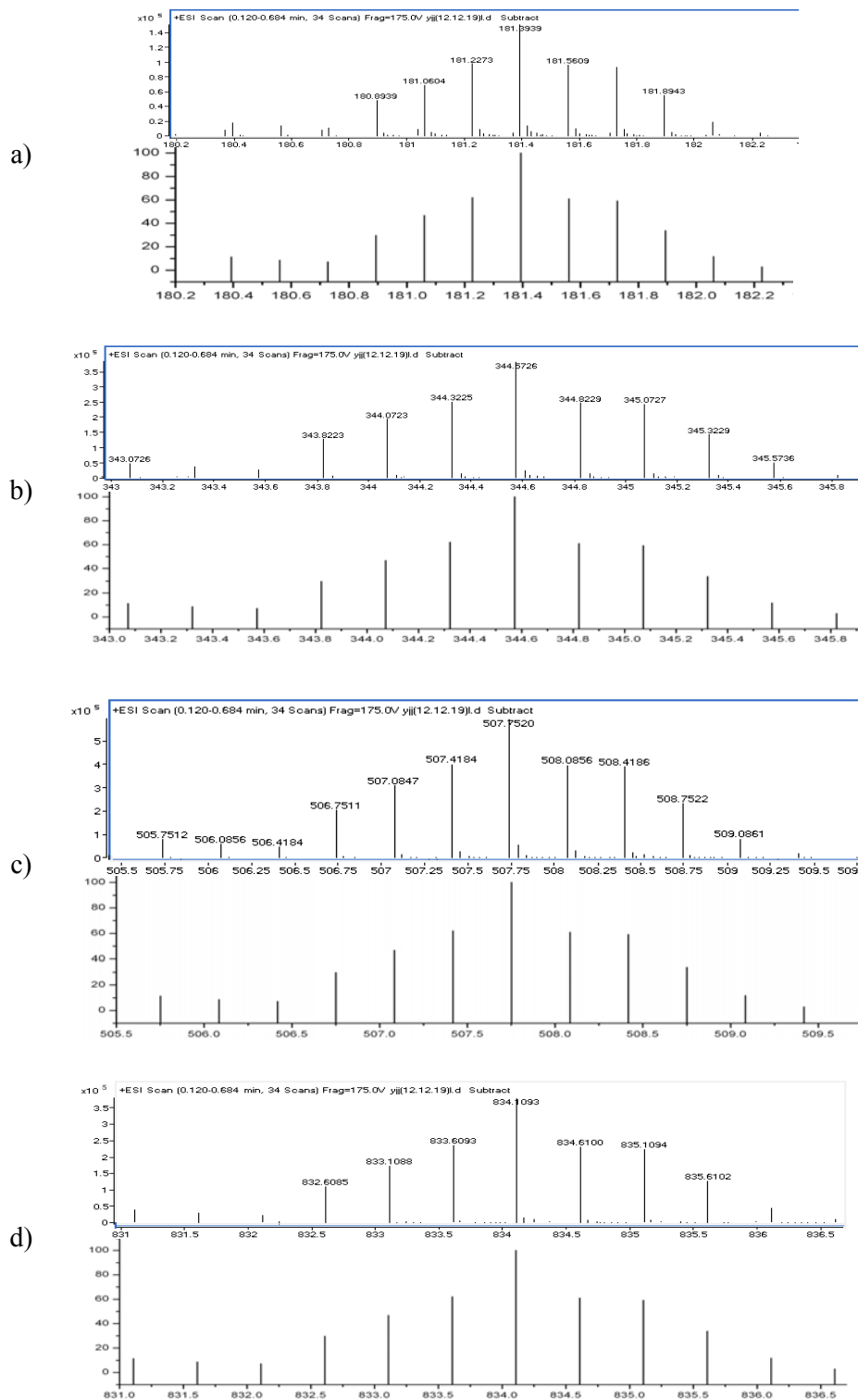
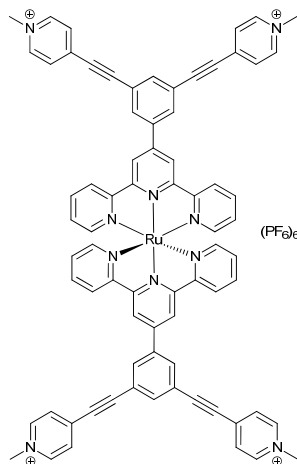


Figure S30 High resolution ESI-MS spectrum of compound $[\text{Ru}(\mathbf{3a})_2][\text{PF}_6]_6$ of signals corresponding to a) $[\text{M}-6\text{PF}_6]^{6+}$, b) $[\text{M}-4\text{PF}_6]^{4+}$, c) $[\text{M}-3\text{PF}_6]^{3+}$ d) $[\text{M}-2\text{PF}_6]^{2+}$

5.1.2 Synthesis and Characterisation of [Ru(4a)₂](PF₆)₆



[Ru(2)₂](PF₆)₂ (20 mg, 0.014 mmol), NH₄PF₆ (60 mg, 0.2 mmol) and methyl iodide (1 mL, 7 mmol) were dissolved in MeCN (30 mL) and heated to reflux overnight to give a red suspension. Water was added to the suspension and the volume reduced under reduced pressure. The suspension was collected on Celite, washed with water, EtOH, DCM and Et₂O. The residue was dissolved in MeCN and the solvent removed to give the title compound [Ru(4a)₂](PF₆)₆ as a red solid (28 mg, 0.014 mmol, 99%). ¹H NMR (500 MHz, CD₃CN) δ 9.11 (s, 2H, H^{B3}), 8.72 (t, *J* = 8.2 Hz, 2H, H^{A3}), 8.71 – 8.65 (m, 6H, H^{D2+C4}), 8.24 (s, 1H, H^{C2}), 8.15 (d, *J* = 6.3 Hz, 4H, H^{D3}), 7.99 (t, *J* = 7.8 Hz, 2H, H^{A4}), 7.47 (d, *J* = 5.4 Hz, 2H, H^{A6}), 7.23 (t, *J* = 6.4 Hz, 2H, H^{A5}), 4.33 (s, 6H, H^{Me}). ¹³C{¹H} NMR (101 MHz, CD₃CN) δ 158.8 (C^{A2}), 156.6 (C^{B2}), 153.4 (C^{A6}), 146.4 (C^{D2}), 146.3 (C^{C5}), 140.2 (C^{D4}), 139.6 (C^{B4}), 139.2 (C^{A4}), 137.8 (C^{C2}), 134.6 (C^{C4}), 130.5 (C^{D3}), 128.6 (C^{A5}), 125.6 (C^{A3}), 123.7 (C^{C1}), 122.7 (C^{B3}), 101.0 (C^{C-alkyne}), 87.1 (C^{D-alkyne}), 49.2 (Me). LR-ESI-MS found *m/z* 197.67 [M-6PF₆]⁶⁺, requires 197.39; 266.25 [M-5PF₆]⁵⁺ requires 265.86; 368.83 [M-4PF₆]⁴⁺ requires 368.57; 539.92 [M-3PF₆]³⁺ requires 539.75; 882.75 [M-2PF₆]²⁺ requires 882.11. HR-ESI-MS found 197.3940 [M-6PF₆]⁶⁺ requires 197.3935; 265.8653 [M-5PF₆]⁵⁺ requires 265.8650, 368.5725; [M-4PF₆]⁴⁺ requires 368.5723; 539.7514 [M-3PF₆]³⁺ requires 539.7511; 882.1099 [M-2PF₆]²⁺ requires 882.1088.

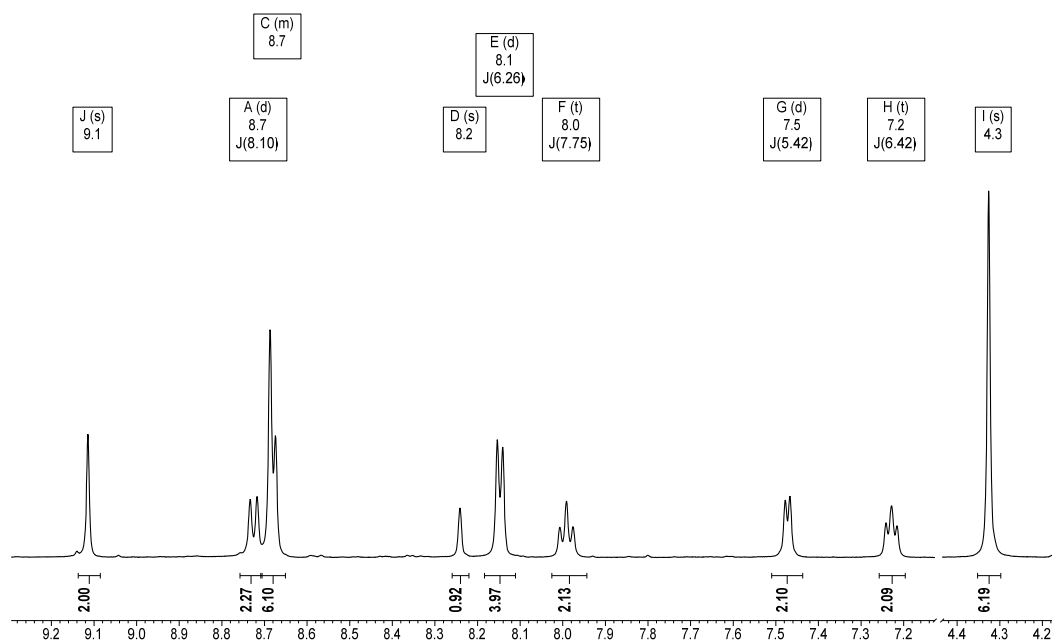


Figure S31 $^1\text{H-NMR}$ (CD_3CN , 500 MHz) of compound $[\text{Ru}(\mathbf{4a})_2][\text{PF}_6]_6$

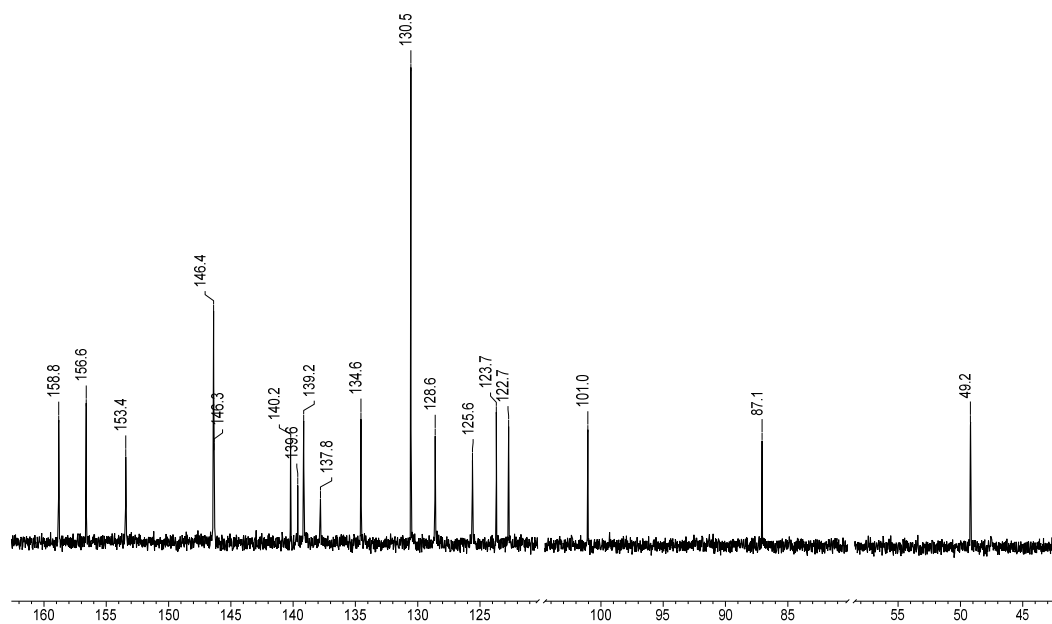


Figure S32 $^{13}\text{C}\{^1\text{H}\}$ -NMR (CD_3CN , 101 MHz) of compound $[\text{Ru}(\mathbf{4a})_2][\text{PF}_6]_6$

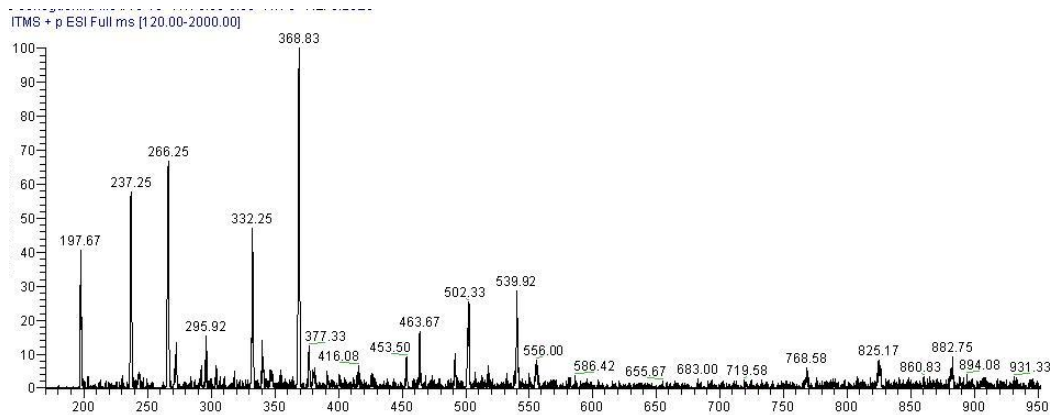


Figure S33 Low resolution ESI-MS spectrum of compound $[\text{Ru}(\mathbf{4a})_2][\text{PF}_6]_6$

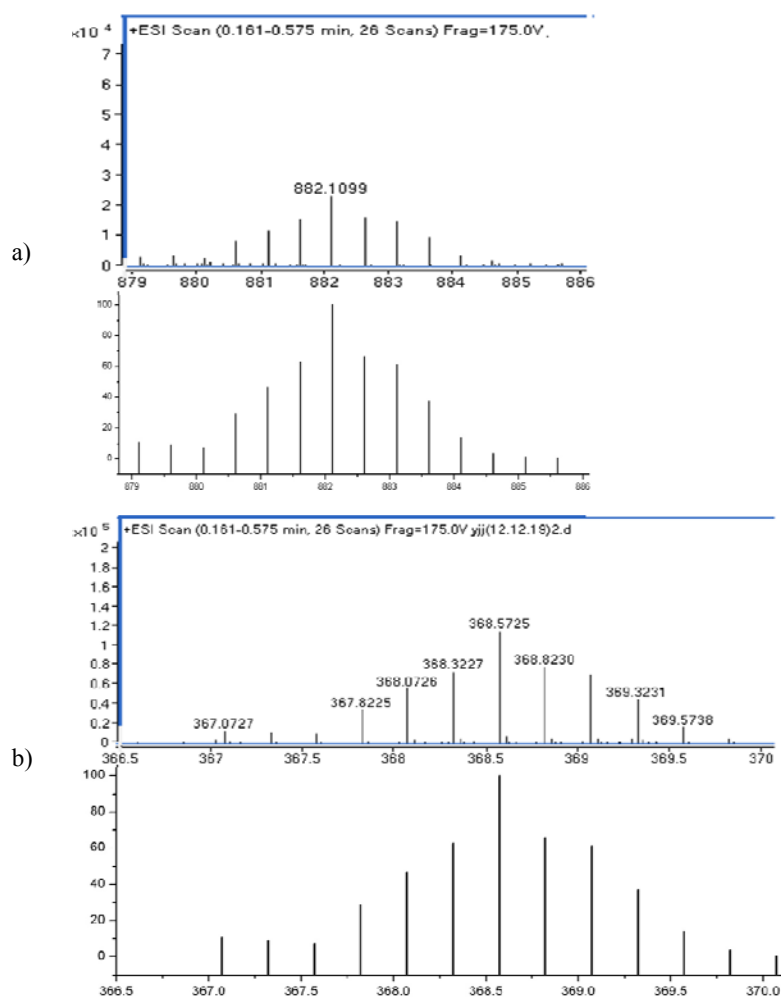
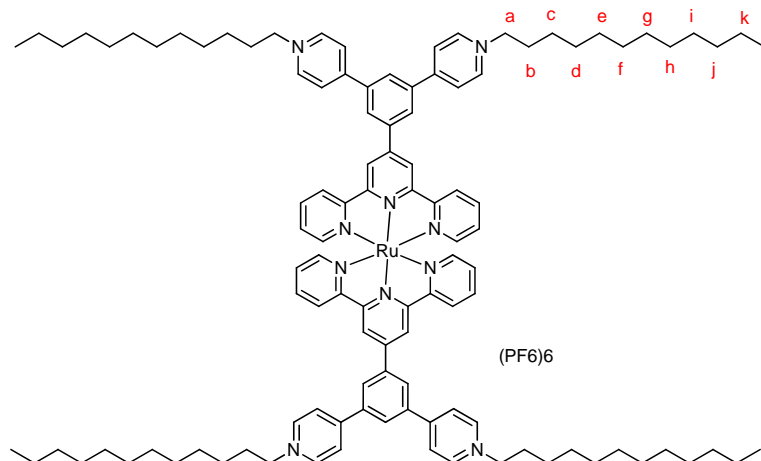


Figure S34 High resolution ESI-MS of compound $[\text{Ru}(\mathbf{4a})_2][\text{PF}_6]_6$ with calculated spectra below, of signals corresponding to a) $[\text{M}-2\text{PF}_6]^{2+}$, b) $[\text{M}-4\text{PF}_6]^{4+}$.

5.1.3 Synthesis and Characterisation of [Ru(3b)₂](PF₆)₆



[Ru(1)₂](PF₆)₂ (20 mg, 0.015 mmol), NH₄PF₆ (60 mg, 0.2 mmol) and 1-bromododecane (3 mL, 10 mmol) were dissolved in MeCN (30 mL) and heated at reflux for 12 h. The solvent was removed under reduced pressure and the crude red powder was purified by column chromatography (SiO₂, MeCN: H₂O: saturated aqueous KNO₃ 14 : 1 : 1). The centre of the main red band was collected, excess aqueous NH₄PF₆ was added and the volume reduced to precipitate the hexafluorophosphate salt which was collected on Celite and washed with water EtOH and Et₂O. The complex was dissolved in DCM and hexane was added to precipitate the complex, which was collected on Celite and washed well with hexane. The residue was dissolved in MeCN and the solvent removed to give the title compound [Ru(3b)₂](PF₆)₆ as a red solid (20 mg, 0.008 mmol, 53%). ¹H NMR (500 MHz, CD₃CN) δ 9.22 (s, 2H, H^{B3}), 9.01 – 8.84 (m, 6H, H^{C4+D2}), 8.76 (d, *J* = 8.1 Hz, 2H, H^{A3}), 8.66 (d, *J* = 6.5 Hz, 4H, H^{D3}), 8.61 (s, 1H, H^{C2}), 8.01 (t, *J* = 7.8 Hz, 2H, H^{A4}), 7.50 (d, *J* = 5.5 Hz, 2H, H^{A6}), 7.25 (t, *J* = 6.5 Hz, 2H, H^{A5}), 4.63 (t, *J* = 7.5 Hz, 4H, H^a), 2.15 – 2.00 (m, 4H, H^b), 1.49 – 1.36 (m, 4H, H^{alk}), 1.37 – 1.22 (m, 14H, H^{alk}), 0.88 (t, *J* = 6.7 Hz, 6H, H^l) (H^{alk} = H^{c-k}). ¹³C{¹H} NMR (126 MHz, CD₃CN) δ 158.9 (C^{A2}), 156.6 (C^{B2}), 155.6 (C^{C1}), 153.4 (C^{A6}), 146.8 (C^{C5}), 145.7 (C^{D2}), 140.8 (C^{B4}), 139.2 (C^{A4}), 137.8 (C^{D4}), 131.4 (C^{C4}), 130.1 (C^{C2}), 128.6 (C^{A5}), 127.0 (C^{D3}), 125.7 (C^{A3}), 123.0 (C^{B3}), 62.4 (C^a), 32.5 (C^j), 31.8 (C^b), 30.2 (C^{alk} x 2), 30.1 (C^{alk}), 30.0 (C^{alk} x 2), 29.6 (C^{alk}), 26.6 (C^c), 23.3 (C^k), 14.3 (C^l). (C^{alk} = C^{d-i}). LR-ESI-MS found *m/z* 284.75 [M-6PF₆]⁶⁺, requires 284.17, *m/z* 370.33 [M-5PF₆]⁵⁺ requires 370.00, *m/z* 499.17 [M-4PF₆]⁴⁺ requires 498.74, *m/z* 713.50 [M-3PF₆]³⁺ requires 713.31, *m/z* 1142.58 [M-2PF₆]²⁺ requires 1142.45; HR-ESI-MS found, 370.0033 [M-5PF₆]⁵⁺ requires 370.0027, 498.7446 [M-4PF₆]⁴⁺ requires 498.7445, 713.3148 [M-3PF₆]³⁺ requires 713.3140, 1142.4516 [M-2PF₆]²⁺ requires 1142.4531.

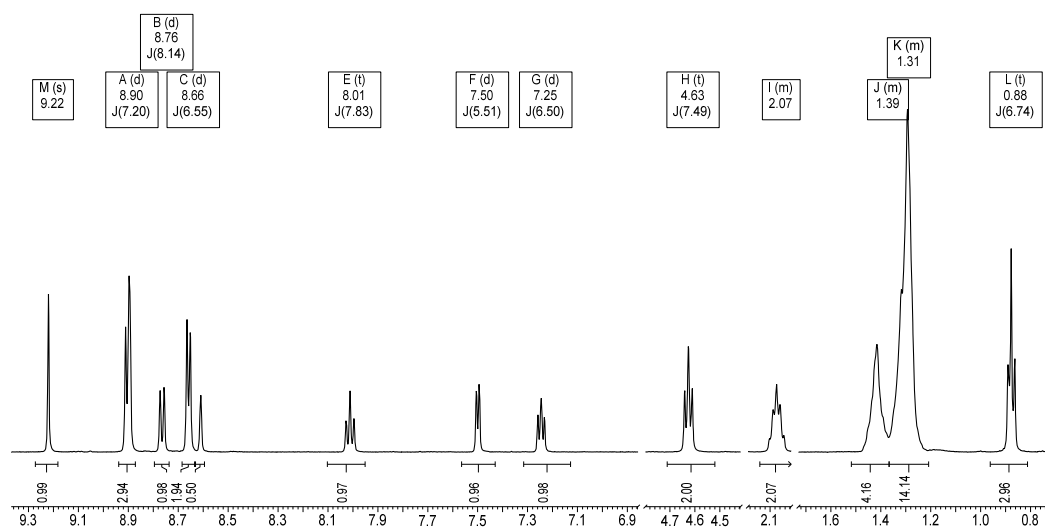


Figure S35 $^1\text{H-NMR}$ (CD_3CN , 500 MHz) of compound $[\text{Ru}(\mathbf{3b})_2][\text{PF}_6]_6$

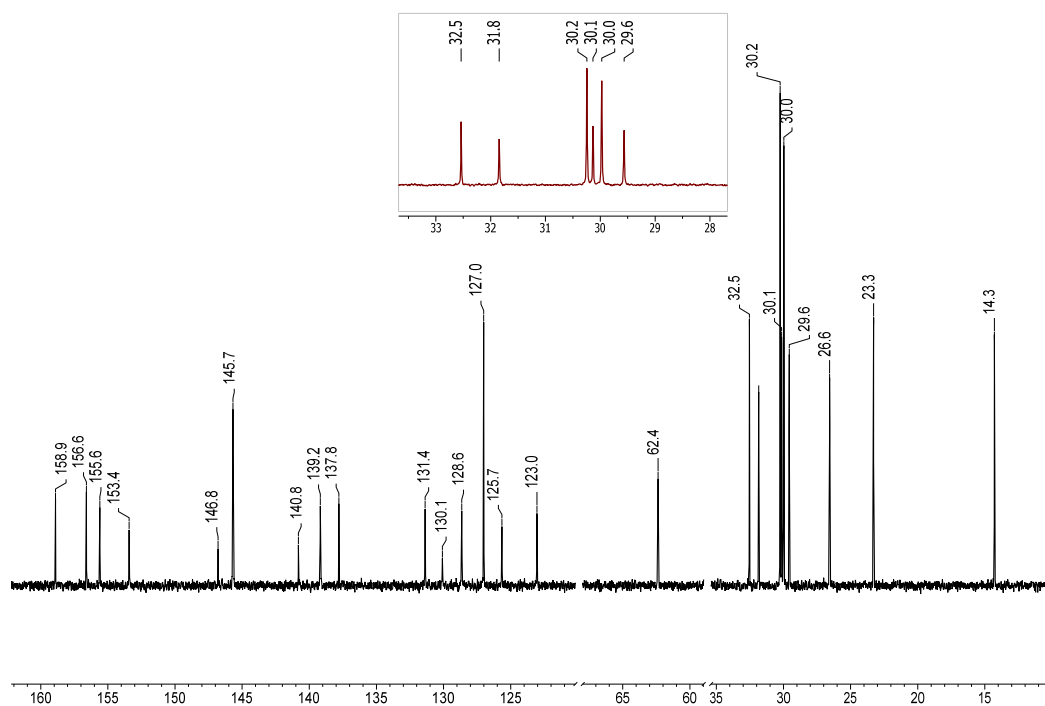


Figure S36 $^{13}\text{C}\{^1\text{H}\}$ -NMR (CD_3CN , 126 MHz) of compound $[\text{Ru}(\mathbf{3b})_2][\text{PF}_6]_6$

D:\test\...2013-01-04\c12-suzuki

1/4/2013 4:19:59 PM

c12-suzuki #19-20 RT: 0.08-0.08 AV: 2 NL: 5.45E3
T: ITMS + p ESI Full ms [200.00-1500.00]

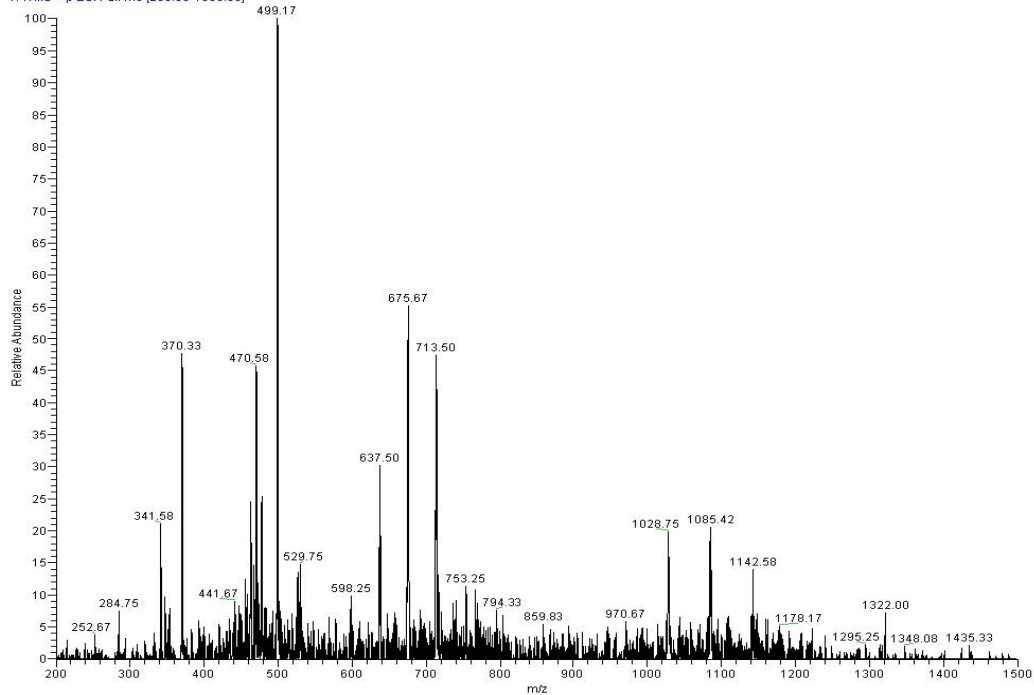


Figure S37 Low resolution ESI-MS spectrum of compound [Ru(3b)₂][PF₆]₆

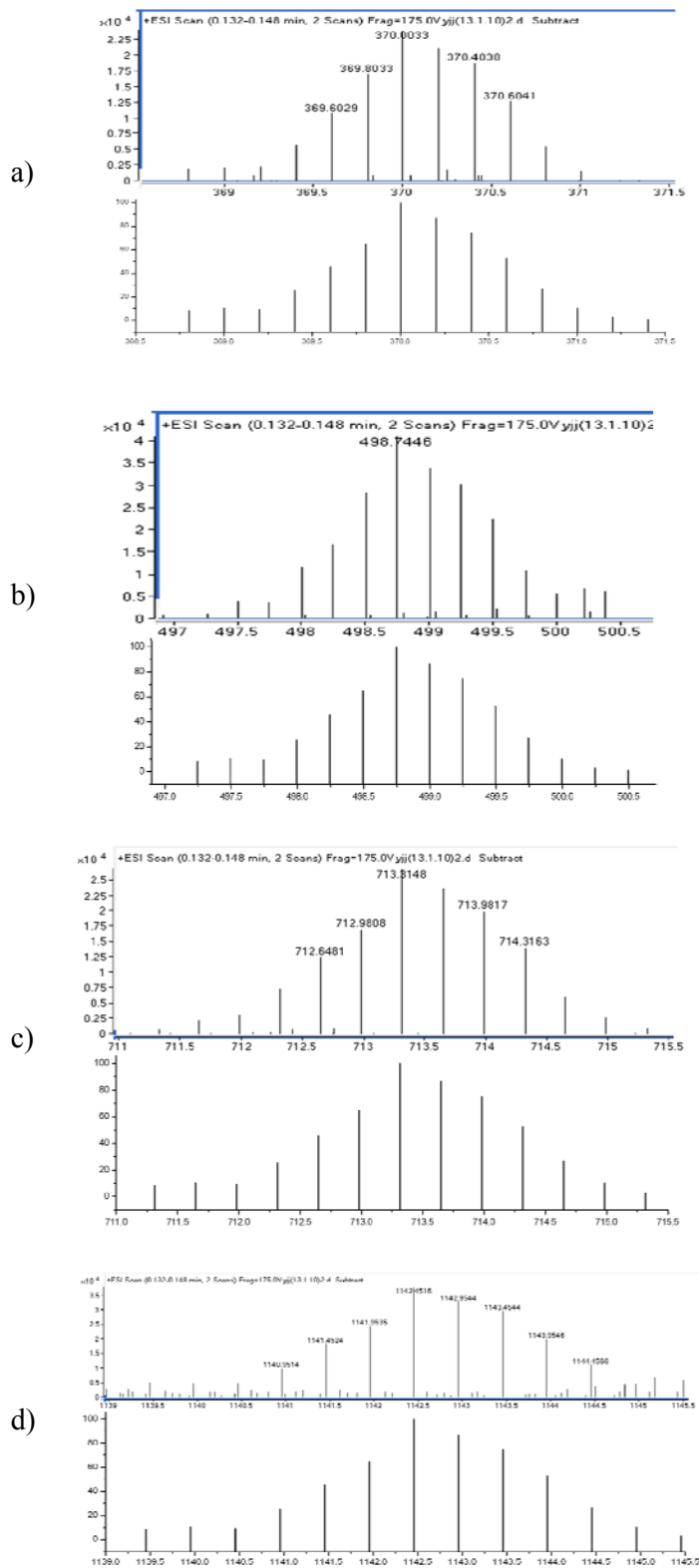
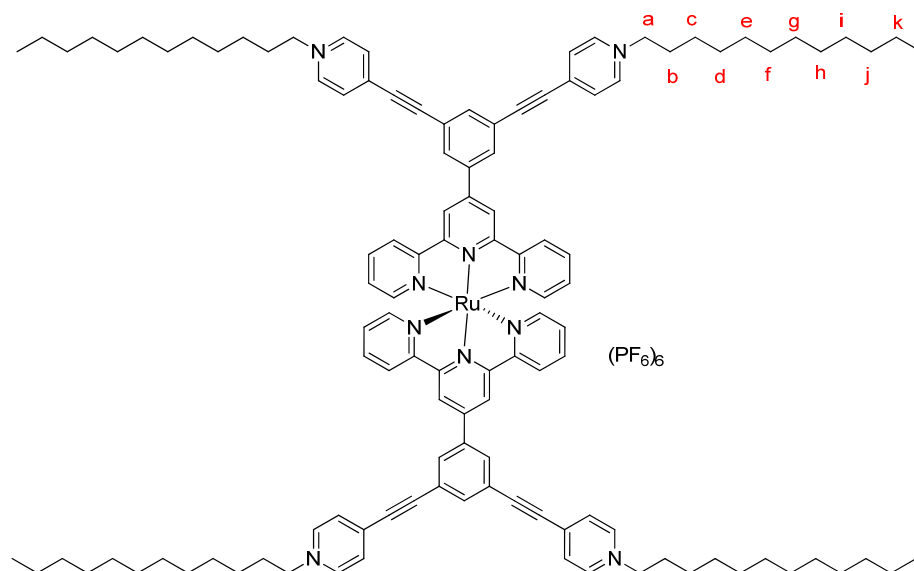


Figure S38 High resolution ESI-MS of compound $[Ru(\mathbf{3b})_2][PF_6]_6$ with calculated spectra below, of signals corresponding to a) $[M-5PF_6]^{5+}$, b) $[M-4PF_6]^{4+}$, c) $[M-3PF_6]^{3+}$ d) $[M-2PF_6]^{2+}$

5.1.4 Synthesis and Characterisation of [Ru(4b)₂](PF₆)₆



[Ru(2)₂](PF₆)₂ (20 mg, 0.014 mmol), NH₄PF₆ (60 mg, 0.2 mmol) and 1-bromododecane (3 mL, 10 mmol) were dissolved in MeCN (30 mL) and DCM (5 mL), heated at reflux for 24h. The solvent was removed under reduced pressure and the crude red powder was purified by column chromatography (SiO₂, MeCN). The centre of the main red band was collected, excess aqueous NH₄PF₆ was added and the volume reduced to precipitate the hexafluorophosphate salt which was collected on Celite and washed with a lot of water, EtOH and hexane. The residue was dissolved in MeCN and the solvent removed to give the title compound [Ru(4b)₂](PF₆)₆ as a red solid (18 mg, 0.007 mmol, 50%). ¹H NMR (400 MHz, CD₃CN) δ 9.10 (s, 1H, H^{B3}), 8.76 – 8.64 (m, 4H, H^{A3+C4+D2}), 8.24 (s, 1H, H^{C2}), 8.16 (d, *J* = 6.8 Hz, 2H, H^{D3}), 7.99 (t, *J* = 7.9 Hz, 1H, H^{A4}), 7.47 (d, *J* = 5.0 Hz, 1H, H^{A6}), 7.23 (ddd, *J* = 7.4, 5.6, 1.1 Hz, 1H, H^{A5}), 4.53 (t, *J* = 7.5 Hz, 2H, H^a), 1.45 – 1.23 (m, 19H, H^{alk}), 0.88 (t, *J* = 6.8 Hz, 3H, H^l) (H^{alk} = H^{b-k}). ¹³C {¹H} NMR (101 MHz, CD₃CN) δ 158.9 (C^{A2}), 156.7 (C^{B2}), 153.5 (C^{A6}), 146.4 (C^{C5}), 145.5 (C^{D2}), 140.5 (C^{D4}), 139.7 (C^{B4}), 139.2 (C^{A4}), 137.9 (C^{C2}), 134.7 (C^{C4}), 131.0 (C^{D3}), 128.7 (C^{A5}), 125.7 (C^{A3}), 123.8 (C^{C1}), 122.8 (C^{B3}), 101.2 (C^{C-alkyne}), 87.2 (C^{D-alkyne}), 62.8 (C^a), 32.6 (C^{alk}), 31.8 (C^b), 30.3 (C^{alk} x 2), 30.2 (C^{alk}), 30.0 (C^{alk} x 2), 29.6 (C^{alk}), 26.5 (C^c), 23.4 (C^k), 14.3 (C^l). (C^{alk} = C^{d-i}). LR-ESI-MS found *m/z* 300.10 [M-6PF₆]⁶⁺, requires 300.17; 389.92 [M-5PF₆]⁵⁺ requires 389.20; 523.08 [M-4PF₆]⁴⁺ requires 522.74; 746.17 [M-3PF₆]³⁺ requires 745.31; 1191.00 [M-2PF₆]²⁺ requires 1190.45. HR-ESI-MS found 300.1753 [M-6PF₆]⁶⁺ requires 300.1749; 389.2048 [M-5PF₆]⁵⁺ requires 389.2027; 522.7470 [M-4PF₆]⁴⁺ requires 522.7444; 745.3170 [M-3PF₆]³⁺ requires 745.3140; 1190.4540 [M-2PF₆]²⁺ requires 1190.4531.

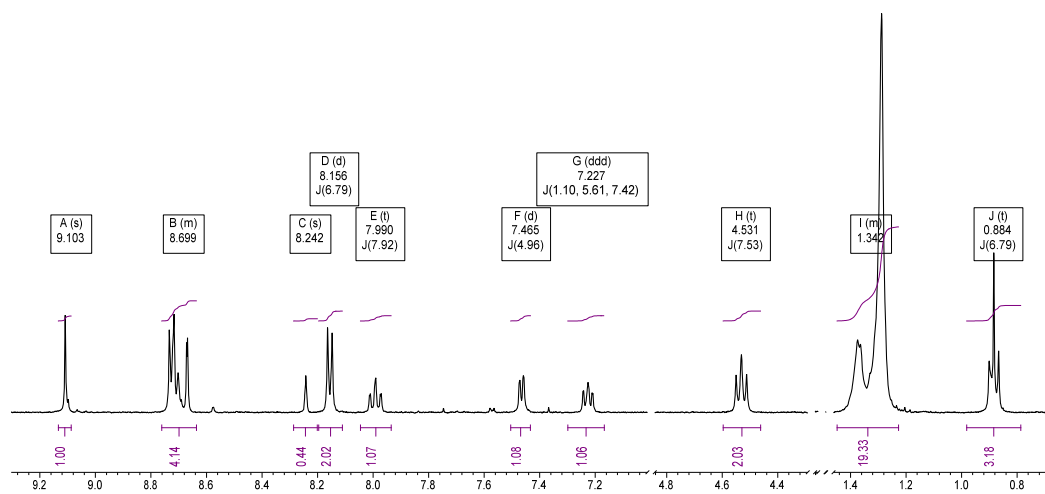


Figure S39 $^1\text{H-NMR}$ (CD_3CN , 500 MHz) of compound $[\text{Ru}(\mathbf{4b})_2][\text{PF}_6]_6$

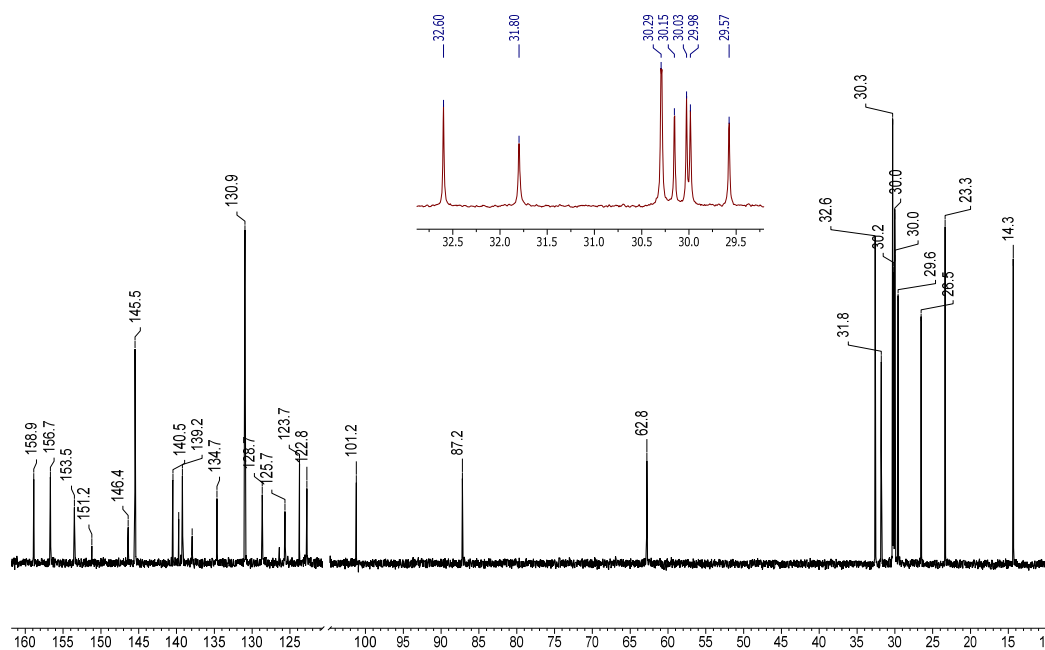


Figure S40 $^{13}\text{C}\{^1\text{H}\}$ -NMR (CD_3CN , 126 MHz) of compound $[\text{Ru}(\mathbf{4b})_2][\text{PF}_6]_6$

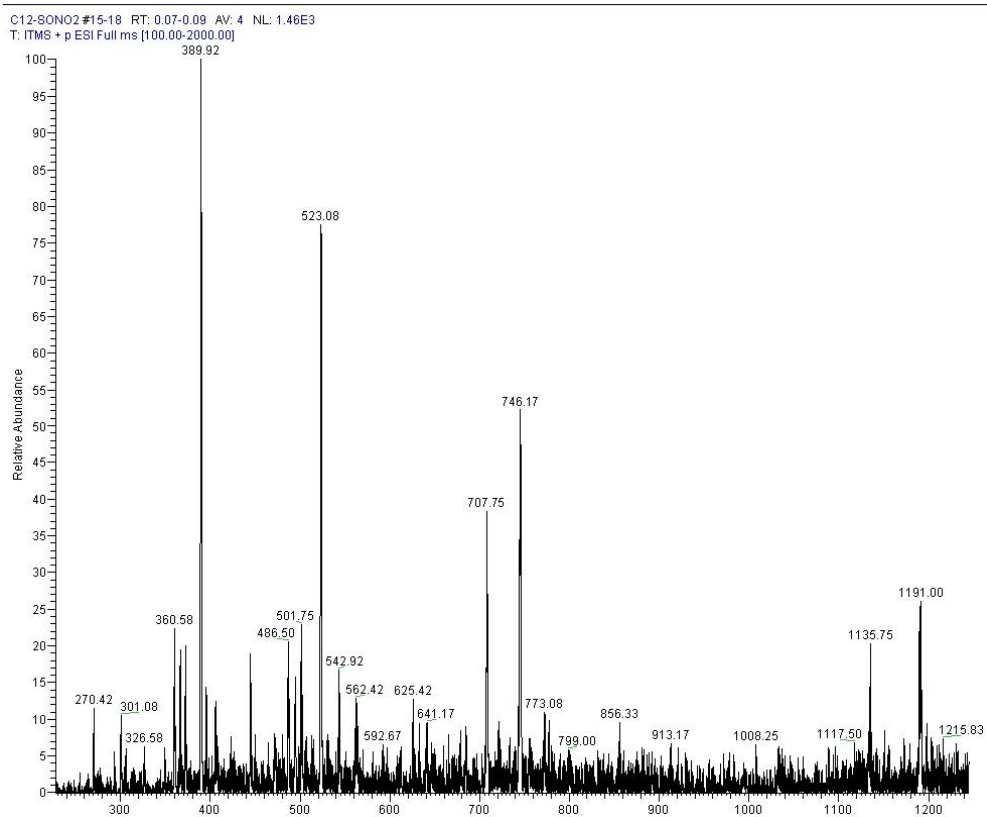


Figure S41 Low resolution ESI-MS spectrum of compound $[\text{Ru}(\mathbf{4b})_2][\text{PF}_6]_6$

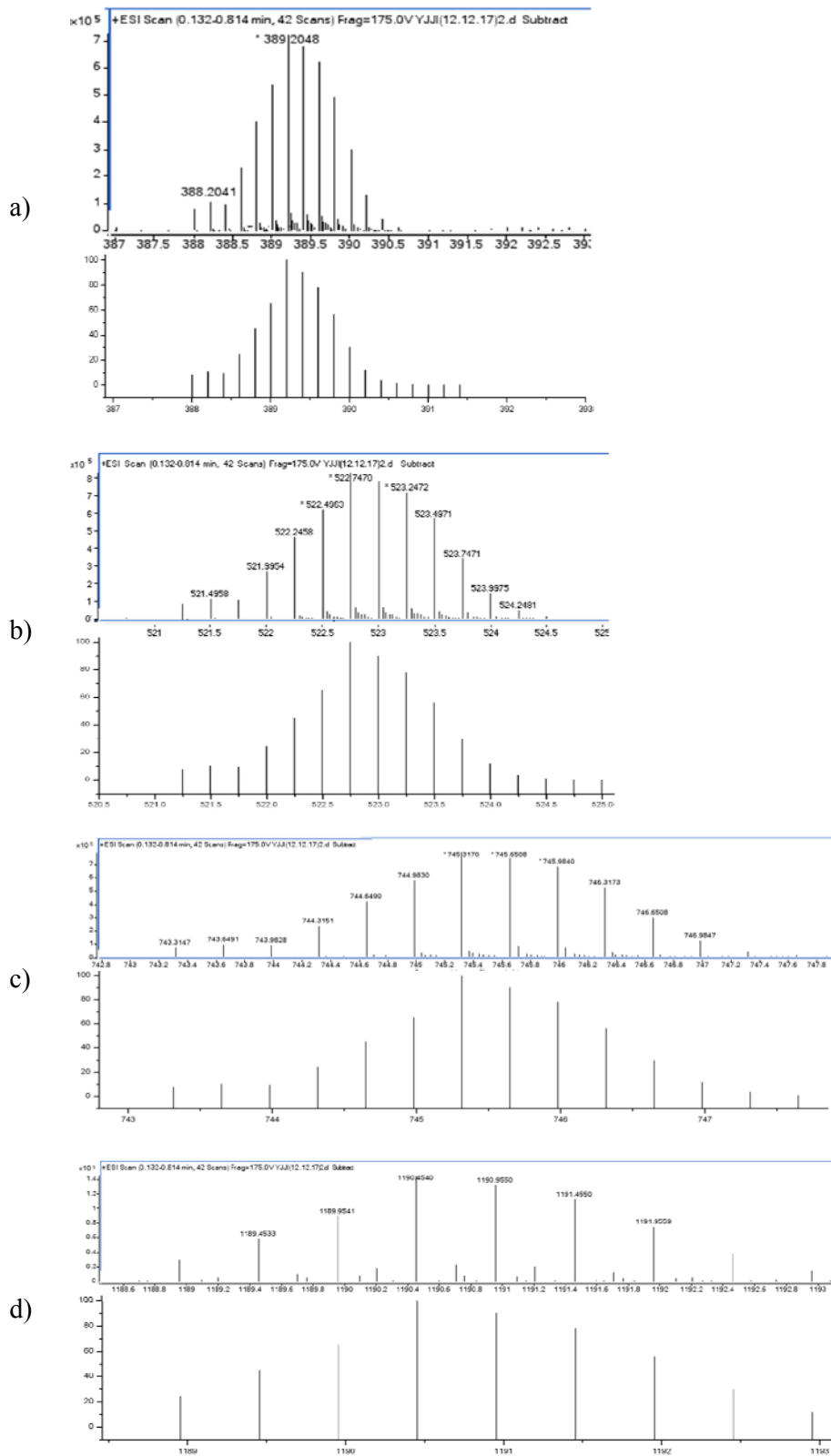


Figure S42 High Resolution ESI-MS spectrum of compound $[\text{Ru}(4\text{b})_2][\text{PF}_6]_6$ with selected peak expansions for a) $[\text{M}-5\text{PF}_6]^{5+}$, b) $[\text{M}-4\text{PF}_6]^{4+}$, c) $[\text{M}-3\text{PF}_6]^{3+}$ and d) $[\text{M}-2\text{PF}_6]^{2+}$ with calculated patterns below

S6. Summary of Absorption Data

Table 1 Absorption spectroscopic data for $[\text{ML}_2](\text{PF}_6)_2$ (; M = Fe, Ru; L = **1**, **2**, **3**) in CH_3CN . Absorption data for $[\text{Fe}(\text{tpy})_2]^{2+}$ and $[\text{Ru}(\text{tpy})_2]^{2+}$ are from ref^[7-8].

	Absorption λ_{max} (ϵ_{max}) nm ($10^3 \text{ dm}^3 \text{ mol}^{-1} \text{ cm}^{-1}$)			
	$\pi^* \leftarrow \pi$			MLCT
$[\text{Fe}(\text{tpy})_2](\text{PF}_6)_2$ ⁷				552
$[\text{Fe}(\text{Phtpy})_2](\text{PF}_6)_2$		284(93)	322(55)	565(27)
$[\text{Fe}(\mathbf{1})_2](\text{PF}_6)_2$	276(71)	285(82)	320(41)	568(22)
$[\text{Fe}(\mathbf{2})_2](\text{PF}_6)_2$		286(122)	299(111)	322(40)
$[\text{Ru}(\text{tpy})_2](\text{PF}_6)_2$ ⁸				475
$[\text{Ru}(\text{Phtpy})_2](\text{PF}_6)_2$				487(26) ⁹
$[\text{Ru}(\mathbf{1})_2](\text{PF}_6)_2$	276(77)	283(80)	311(56)	330(36)
$[\text{Ru}(\mathbf{2})_2](\text{PF}_6)_2$		285(112)	298(108)	330(33)
$[\text{Ru}(\mathbf{3a})_2](\text{PF}_6)_2$		287(151)		332(39)
$[\text{Ru}(\mathbf{4a})_2](\text{PF}_6)_2$		284(107)	313(151)	327(147)
$[\text{Ru}(\mathbf{3b})_2](\text{PF}_6)_2$		288(170)		332(41)
$[\text{Ru}(\mathbf{4b})_2](\text{PF}_6)_2$		285(112)	314(156)	328(153)

tpy = 2,2':6',2''-terpyridine. Phtpy = 4'-phenyl-2, 2':6',2''-terpyridine.

S7. Electrochemical Data

All Electrochemical measurements were conducted in freshly distilled acetonitrile with 0.1M $N^nBu_4PF_6$ electrolyte solution using a CHI600D instrument made by Chinese Shanghai Chenhua instrument co., with a glassy carbon working electrode, platinum counter electrode, Ag wire as a pseudo-reference and calibrated with internal ferrocene added at the end of the experiment.

7.1.1 Cyclic Voltammograms of $[Fe(1)_2](PF_6)_2$ and $[Ru(1)_2](PF_6)_2$

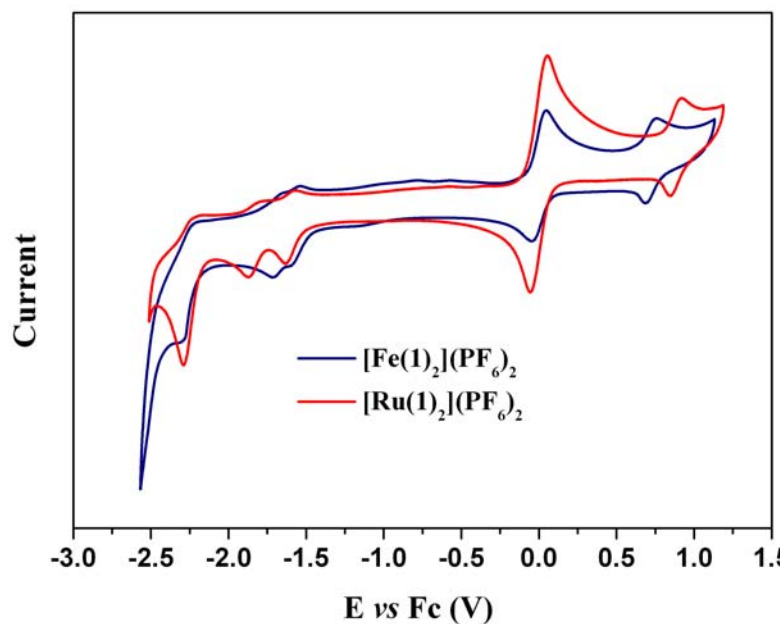


Figure S43 CV (MeCN, 0.1M TBAPF₆) of $[Ru(1)_2](PF_6)_2$ and $[Ru(1)_2](PF_6)_2$ referenced with internal ferrocene.

7.1.2 Cyclic Voltammograms of $[\text{Fe}(\mathbf{2})_2](\text{PF}_6)_2$ and $[\text{Ru}(\mathbf{2})_2](\text{PF}_6)_2$

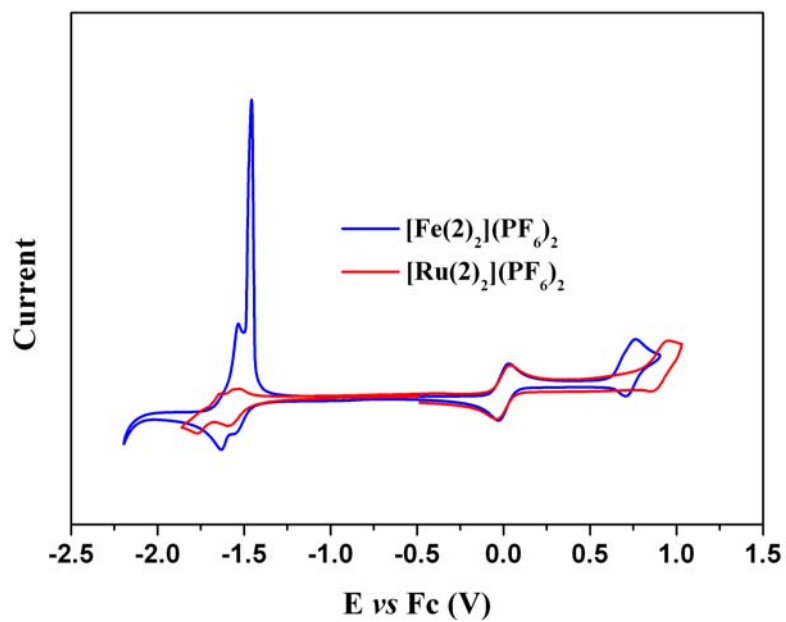


Figure S44 CV (MeCN, 0.1M TBAPF₆) of $[\text{Fe}(\mathbf{2})_2](\text{PF}_6)_2$ and $[\text{Ru}(\mathbf{2})_2](\text{PF}_6)_2$ referenced with internal ferrocene.

7.1.3 Cyclic Voltammograms of *N*-Me complexes $[\text{Ru}(\mathbf{3a})_2](\text{PF}_6)_6$ and $[\text{Ru}(\mathbf{4a})_2](\text{PF}_6)_6$

The CV data is plotted with the parent (ie: non-methylated) complexes for comparison.

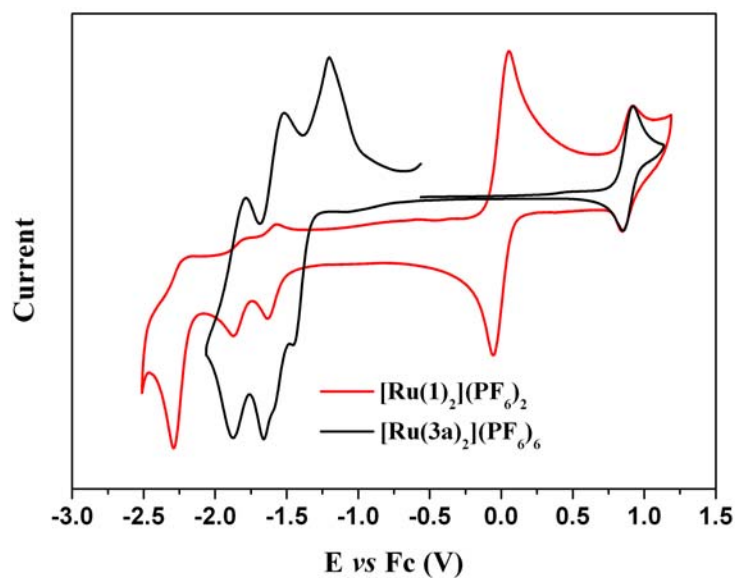


Figure S45 CV (MeCN, 0.1M TBAPF₆) of $[\text{Ru}(\mathbf{1})_2](\text{PF}_6)_2$ and $[\text{Ru}(\mathbf{3a})_2](\text{PF}_6)_6$ referenced with internal ferrocene.

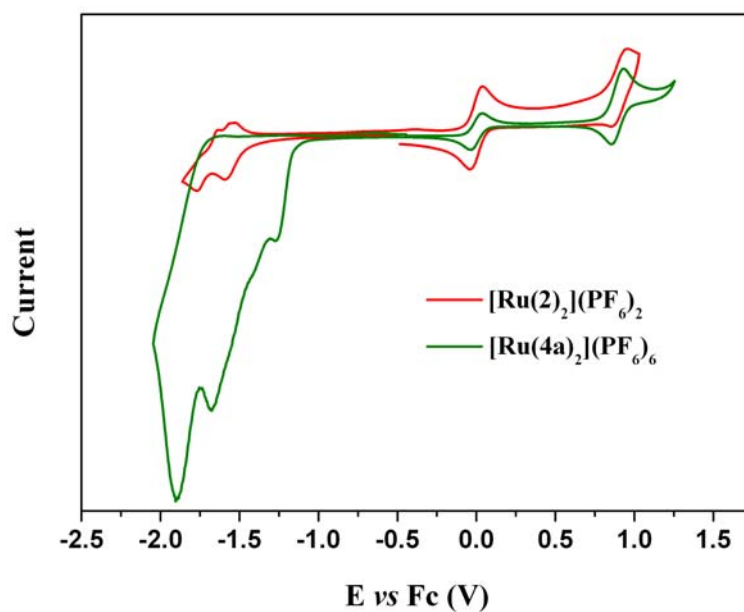


Figure S46 CV (MeCN, 0.1M TBAPF₆) of $[\text{Ru}(\mathbf{2})_2](\text{PF}_6)_2$ and $[\text{Ru}(\mathbf{4a})_2](\text{PF}_6)_6$ referenced with internal ferrocene.

7.1.4 Cyclic Voltammograms of *N*-C₁₂H₂₅ complexes [Ru(3b)₂](PF₆)₆ and [Ru(4b)₂](PF₆)₆

The CV data is plotted with the parent (ie: non-alkylated) complexes and the simple *N*-Me analogues for comparison. CV spectra of *N*-methyl and *N*-C₁₂H₂₅ derivatives were very similar, as expected.

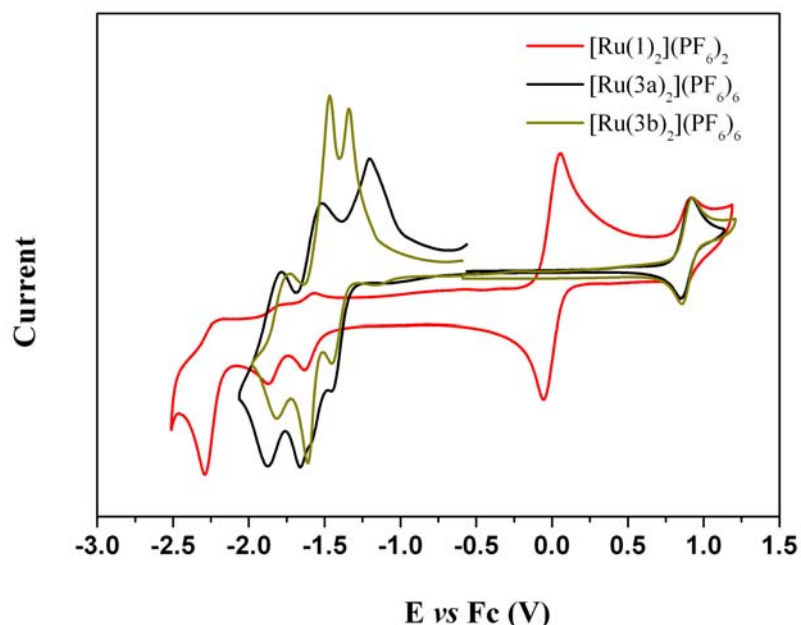


Figure S47 CV (MeCN, 0.1M TBAPF₆) of [Ru(1)₂](PF₆)₂ and [Ru(3a)₂](PF₆)₆ and [Ru(3b)₂](PF₆)₆ referenced with internal ferrocene.

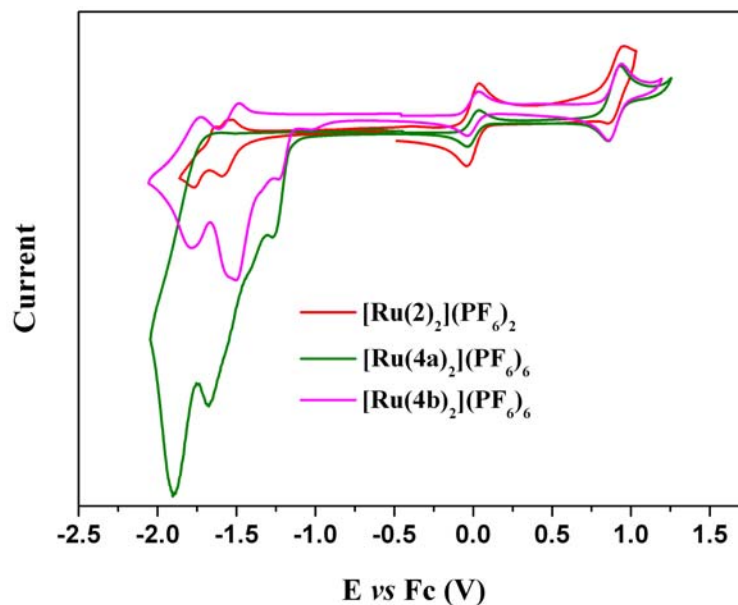


Figure S48 CV (MeCN, 0.1M TBAPF₆) of [Ru(2)₂](PF₆)₂ and [Ru(4a)₂](PF₆)₆ and [Ru(4b)₂](PF₆)₆ referenced with internal ferrocene.

7.1.5 Electrochemical data for [Fe(4'-phenyl-(2,2':6',6''-terpyridine)₂](PF₆)₂

4-phenyltpy was prepared by literature methods,¹ and the Fe(II) complex was prepared analogous to that for [Fe(**1**)₂](PF₆)₂.

¹H NMR (400 MHz, CD₃CN) δ 9.20 (s, 2H, H^{B3}), 8.62 (d, *J* = 8.0 Hz, 2H, H^{A3}), 8.33 (d, *J* = 7.3 Hz, 2H, H^{C2}), 7.91 (td, *J* = 7.9, 1.4 Hz, 2H, H^{A4}), 7.82 (t, *J* = 7.5 Hz, 2H, H^{C3}), 7.74 (t, *J* = 7.4 Hz, 1H, H^{C4}), 7.20 (d, *J* = 5.2 Hz, 2H, H^{A6}), 7.09 (ddd, *J* = 7.0, 5.7, 1.1 Hz, 2H, H^{A5}). ¹³C{¹H} NMR (101 MHz, CD₃CN) δ 161.2 (C^{B2}), 159.0 (C^{A2}), 154.0 (C^{A6}), 151.4 (C^{B4}), 139.7 (C^{A4}), 137.7 (C^{C1}), 131.6 (C^{C4}), 130.7 (C^{C3}), 128.8 (C^{C2}), 128.2 (C^{A5}), 124.7 (C^{A3}), 122.6 (C^{B3}).

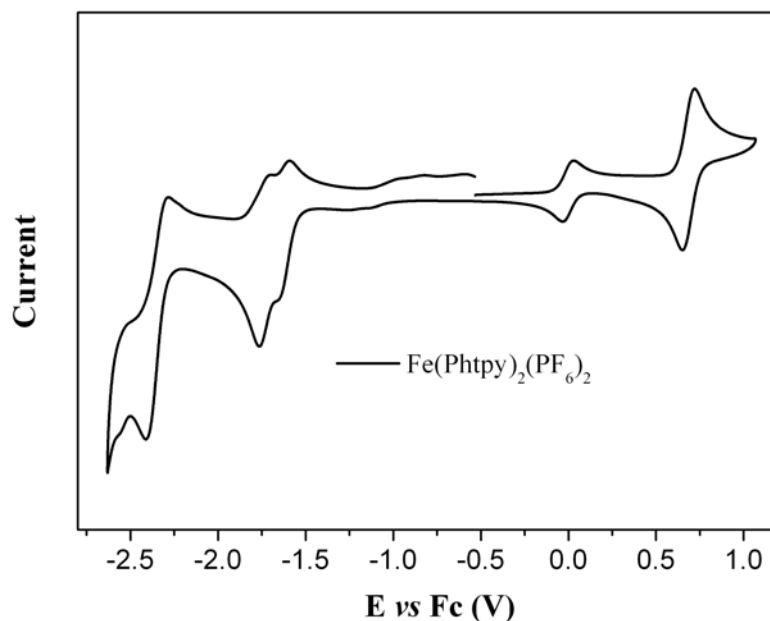


Figure S49 CV (MeCN, 0.1M TBAPF₆) of [Fe(Phtpy)₂](PF₆)₂ referenced with internal ferrocene. Phtpy = 4'-phenyl-2,2':6',6''-terpyridine,

7.1.6 Differential Pulse Voltammetry (DPV) for $[\text{Ru}(\mathbf{1})_2](\text{PF}_6)_2$, $[\text{Ru}(\mathbf{3a})_2](\text{PF}_6)_6$ and $[\text{Ru}(\mathbf{3b})_2](\text{PF}_6)_6$

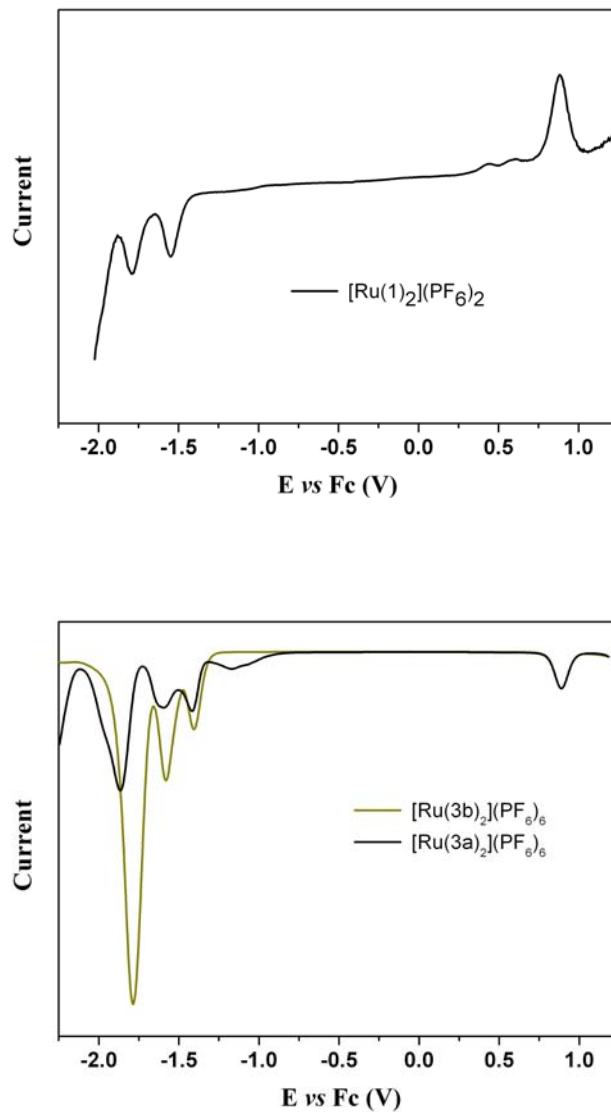


Figure S50 Differential Pulse Voltammetry (DPV) (MeCN, 0.1M TBAPF₆) of a) $[\text{Ru}(\mathbf{1})_2](\text{PF}_6)_6$ (combined positive and negative DPV) and b) $[\text{Ru}(\mathbf{3a})_2](\text{PF}_6)_6$, $[\text{Ru}(\mathbf{3b})_2](\text{PF}_6)_6$ (normalized for Ru^{2+/3+} peak, single DPVs) referenced with internal ferrocene in a subsequent scan.

7.1.7 Summary of electrochemical data

Table S2 Electrochemical data^a

	M ^{2+/3+} (V)	Ligand reductions ^b (V)			λ _{max} (nm) MLCT
[Fe(tpy) ₂](PF ₆) ₂ ⁷	+0.74	-1.64		-1.82	552 ⁷
[Fe(tpyPh) ₂](PF ₆) ₂ ^c	+0.69	-1.62	-1.73	-2.34	565
[Fe(tpypy) ₂](PF ₆) ₂ ⁷	+0.80	-1.51	-1.66		569 ⁸
[Fe(1) ₂](PF ₆) ₂	+0.72	-1.57	-1.68	-2.25	568
[Fe(2) ₂](PF ₆) ₂	+0.73	-1.51 ^{qr}	-1.54 ^{red}	-1.63 ^{red} -1.58 ^{qr}	569
			/-1.45 ^{abs/reox}	/-1.53 ^{reox}	
[Ru(tpy) ₂](PF ₆) ₂ ⁹	+0.92	-1.67		-1.92	475 ⁸
[Ru(tpyPh) ₂](PF ₆) ₂ ^{8,9}	+0.90	-1.66		-1.92	487 ^{8,9}
[Ru(tpypy) ₂](PF ₆) ₂ ¹⁰	+0.95	-1.54		-1.80	492 ¹⁰
[Ru(tpypyN-Me) ₂](PF ₆) ₂ ¹⁰	+1.03	-1.06	-1.56	-1.79	507 ¹⁰
		-1.16			
[Ru(1) ₂](PF ₆) ₂	+0.89	-1.60	-1.84	-2.26	489
[Ru(2) ₂](PF ₆) ₂	+0.91	-1.55	-1.77 ^{qr}	-1.56 ^{abs} -1.63 ^{reox}	490
[Ru(3a) ₂](PF ₆) ₂	+0.89	-1.20 ^{abs}	-1.42	-1.54	491
				-1.66 ^{qr} -1.83 -2.28 ^{irr}	
[Ru(3b) ₂](PF ₆) ₂	+0.89	-1.40		-1.61 ^{qr} -1.77	491
[Ru(4a) ₂](PF ₆) ₂ ^d	+0.89	-1.26 ^{irr}	-1.67 ^{qr, d}	-1.89 ^{irr}	490
[Ru(4b) ₂](PF ₆) ₂	+0.90	-1.24 ^{irr}	-1.51 ^{irr}	-1.54 ^{qr}	491

^a All measurements in MeCN with 0.1M [nBuN]PF₆, with a glassy carbon working electrode, platinum counter electrode, Ag+/AgCl reference and potentials quoted are *versus* Fc+/Fc. tpy = 2,2':6',2''-terpyridine; tpyPh = 4'-phenyl-2,2':6',2''-terpyridine; tpypy = 4'-(4-pyridyl)-2,2':6',2''-terpyridine; tpypyN-Me = N-methyl-(4-pyridium)-2,2':6',2''-terpyridine. ^b All processes are reversibly, except where noted qr = quasi-reversible, irr = irreversible. ^c Data previously reported for [Fe(tpyPh)₂](ClO₄)₂ vs Ag/AgC (ref #¹¹), but measurements were repeated here for [Fe(tpyPh)₂](PF₆)₂ for consistency. ^d Several irreversible processes between -1.5 to -1.9V

S8. X-Ray diffraction experimental

8.1.1 General

Data were collected with ω scans to approximately $56^\circ 2\theta$ using a Bruker-Nonius APEX-II diffractometer employing graphite-monochromated Mo-K α radiation generated from a sealed tube (0.71073 Å) at 293(2) K. Data integration and reduction were undertaken with SAINT and XPREP¹² Subsequent computations were carried out using the WinGX-32 graphical user interface.¹³ Structures were solved by direct methods using SIR97.¹⁴ Multi-scan empirical absorption corrections, when applied, were applied to the data set using either TWINABS or SADABS.¹⁵ Data were refined and extended with SHELXL-97 or SHELXH-97.¹⁶ In general, non-hydrogen atoms with occupancies greater than 0.25 were refined anisotropically. Carbon-bound hydrogen atoms were included in idealised positions and refined using a riding model. Data and specific details (where required) regarding the refinement are given below.

8.1.2 Data for structure [Ru(1)₂]-2PF₆-8.25H₂O

Formula C₆₂H_{58.50}F₁₂N₁₀O_{8.25}P₂Ru, *M* 1466.69, monoclinic, space group C2/c(#15), *a* 32.008(5), *b* 17.136(3), *c* 26.226(5) Å, β 105.545(3), *V* 13858(4) Å³, *D_c* 1.406 g cm⁻³, *Z* 8, crystal size 0.10 by 0.05 by 0.02 mm, colour orange, habit plate, temperature 293(2) Kelvin, λ (MoK α) 0.71073 Å, μ (MoK α) 0.363 mm⁻¹, $T(\text{SADABS})_{\text{min,max}}$ 0.9646, 0.9928, $2\theta_{\text{max}}$ 52.74, *hkl* range -39 39, -21 21, -32 32, *N* 54479, *N_{ind}* 13990 (*R_{merge}* 0.1853), *N_{obs}* 6183 (*I* > 2 σ (*I*)), *N_{var}* 748, residuals * *R*1(*F*) 0.0969, *wR*2(*F*²) 0.2739, GoF(all) 0.946, $\Delta\rho_{\text{min,max}}$ -0.877, 0.986 e⁻ Å⁻³.

* $R1 = \sum ||F_o| - |F_c|| / \sum |F_o|$ for $F_o > 2\sigma(F_o)$; $wR2 = (\sum w(F_o^2 - F_c^2)^2 / \sum (wF_c^2)^2)^{1/2}$ all reflections

$w = 1 / [\sigma^2(F_o^2) + (0.1294P)^2 + 0.0000P]$ where $P = (F_o^2 + 2F_c^2) / 3$

Specific refinement details:

Despite appearing (at least visually) of good quality, the crystals employed displayed poor diffraction properties. The diffraction pattern obtained was broad and very few reflections were observed at better than 0.8 Å resolution. These

properties are due to substantial disorder within the structure and result in a larger than ideal R_{int} . One of the 4-pyridyl groups is disordered and is modelled over two equal occupancy positions with equal thermal parameters; rigid body restraints were required on these two rings to facilitate realistic modelling. The water solvate molecules are also disordered with a total of 4.5 molecules modelled over 10 positions. There is also a substantial region of smeared electron density within the crystal lattice. Despite multiple attempts at modelling this region as a combination of disordered anions and solvent not satisfactory model was obtained and accordingly the structure was treated with the SQUEEZE¹⁷ function of PLATON¹⁸ which resulted in substantially improved residuals. Solvent hydrogen atoms could not be located in the difference Fourier map and were not modelled.

8.1.3 Data for structure [Fe(1)₂]-2PF₆-6MeNO₂-12.5H₂O

Formula C₆₈H₈₁F₁₂FeN₁₆O_{22.50}P₂, M 1828.27, monoclinic, space group $C2/c$ (#15), a 31.977(4), b 16.992(2), c 26.943(3) Å, β 106.844(2), V 14011(3) Å³, D_c 1.733 g cm⁻³, Z 8, crystal size 0.12 by 0.06 by 0.02 mm, colour purple, habit plate, temperature 293(2) Kelvin, $\lambda(\text{MoK}\alpha)$ 0.71073 Å, $\mu(\text{MoK}\alpha)$ 0.389 mm⁻¹, $T(\text{SADABS})_{\text{min,max}}$ 0.9523, 1.0000, $2\theta_{\text{max}}$ 52.74, hkl range -39 39, -21 21, -33 33, N 57055, N_{ind} 14269 (R_{merge} 0.0957), N_{obs} 6998 ($I > 2\sigma(I)$), N_{var} 788, residuals * $R1(F)$ 0.0968, $wR2(F^2)$ 0.3023, GoF(all) 0.966, $\Delta\rho_{\text{min,max}}$ -0.842, 1.027 e⁻ Å⁻³.

* $R1 = \sum ||F_o| - |F_c|| / \sum |F_o|$ for $F_o > 2\sigma(F_o)$; $wR2 = (\sum w(F_o^2 - F_c^2)^2 / \sum (wF_c^2)^2)^{1/2}$ all reflections

$w = 1 / [\sigma^2(F_o^2) + (0.1810P)^2]$ where $P = (F_o^2 + 2F_c^2) / 3$

Specific refinement details:

This complex is essentially isostructural with the ruthenium analogue and suffered from the same poor diffraction properties, including broad and weak reflections. These properties are again due to substantial disorder within the structure. One of the 4-pyridyl groups is disordered and is modelled over two equal occupancy positions with equal thermal parameters; rigid body restraints were required on these two rings to facilitate realistic modelling. The solvate molecules are also disordered with a total of 4.5 water molecules modelled over eight positions. There is also a substantial region of smeared electron density within the crystal lattice. Despite multiple attempts at modelling this region as a combination of disordered anions and solvent not satisfactory model was obtained and accordingly the structure was

treated with the SQUEEZE¹⁷ function of PLATON¹⁸ which resulted in substantially improved residuals. Water-bound hydrogen atoms could not be located in the difference Fourier map and were not modelled.

8.1.4 Data for structure 3 [Ru(1)₂]-5PF₆-NO₃

Formula C₁₈₆H₁₂₆F₃₀N₃₁O₃P₅Ru₃, *M* 3871.23, Triclinic, space group *P*1 (#2), *a* 19.323(5), *b* 20.548(6), *c* 26.542(7) Å, *α* 81.138(5), *β* 81.923(5), *γ* 84.253(5)°, *V* 10276(5) Å³, *D_c* 1.251 g cm⁻³, *Z* 2, crystal size 0.15 by 0.10 by 0.10 mm, colour orange, habit block, temperature 293(2) Kelvin, *λ*(MoKα) 0.71073 Å, *μ*(MoKα) 0.339 mm⁻¹, *T*(TWINABS (SHELDRICK, 2008))_{min,max} 0.358723, 0.428305, *2θ*_{max} 41.63, *hkl* range -19 19, -20 20, 0 26, *N* 21222, *N*_{obs} 12407(*I* > 2σ(*I*)), *N*_{var} 1232, residuals* *R*1(*F*) 0.1204, *wR*2(*F*²) 0.3787, GoF(all) 1.289, Δ*ρ*_{min,max} -0.935, 1.105 e⁻ Å⁻³.

* $R1 = \frac{\sum ||F_o| - |F_c||}{\sum |F_o|}$ for $F_o > 2\sigma(F_o)$; $wR2 = (\frac{\sum w(F_o^2 - F_c^2)^2}{\sum w(F_c^2)^2})^{1/2}$ all reflections

$w = 1/[\sigma^2(F_o^2) + (0.2000P)^2]$ where $P = (F_o^2 + 2F_c^2)/3$

Specific refinement details:

Despite appearing (at least visually) to be single crystals of good quality, the sample employed proved to be a twinned¹⁹ by a two-fold rotation about *c* with approximately equal components. Like the other structures in this series, the data was also broad and weak, reflecting significant disorder. The complex crystallises with three cations within the asymmetric unit and two of the 4-pyridyl groups are disordered and modelled over two equal occupancy positions with equal thermal parameters. Rigid body restraints were also required in a number of aromatic rings to facilitate realistic modelling. Only one hexafluorophosphate and one nitrate anion could be successfully modelled. The remaining electron density (corresponding to anions) was smeared throughout a large cell volume and accordingly was modelled as disordered phosphorous atoms until a plateau of approximately 1 e⁻ Å⁻³ was reached in order to account for this electron density. These problems collectively have resulted in larger than ideal residuals in this structure.

8.1.5 Data for [Ru(2)₂](PF₆)₂-4Et₂O

Formula C₈₆H₈₂F₁₂N₁₀O₄P₂Ru, *M* 1710.63, Orthorhombic, space group *Fddd*(#70), *a* 21.841(3), *b* 25.024(2), *c* 34.582(3) Å, *V* 18900(4) Å³, *D_c* 1.202 g cm⁻³, *Z* 8, crystal size 0.24 by 0.22 by 0.20 mm, colour red, habit block, temperature 293(2) Kelvin, $\lambda(\text{MoK}\alpha)$ 0.71073 Å, $\mu(\text{MoK}\alpha)$ 0.273 mm⁻¹, *T*(SADABS)_{min,max} 0.7, 0.8, $2\theta_{\text{max}}$ 52.00, *hkl* range -26 26, -30 30, -42 38, *N* 37508, *N_{ind}* 4660 (*R_{merge}* 0.0978), *N_{obs}* 2980 (*I* > 2σ(*I*)), *N_{var}* 312, residuals * *R*(*F*²) 0.0537, *R_w*(*F*²) 0.1111, GoF(all) 1.053, $\Delta\rho_{\text{min,max}}$ -0.603, 1.017 e⁻ Å⁻³.

$$*R = \frac{\sum |F_o^2 - F_c^2|}{\sum F_o^2}; R_w = \frac{(\sum w(F_o^2 - F_c^2)^2)^{1/2}}{(\sum wF_c^2)^{1/2}}$$

$$w = 1/[\sigma^2(F_o^2) + (0.04P)^2 + 1.22P] \text{ where } P = (F_o^2 + 2F_c^2)/3$$

Specific collection and refinement details:

A block-like crystal was sealed in a capillary and mounted on a Bruker Smart Apex CCD diffractometer employing graphite monochromated MoK α radiation generated from a sealed tube. Cell constants were obtained from a least squares refinement against 8136 reflections located between 4.94 and 49.96° 2 θ . Data were collected at 293(2) Kelvin with phi and omega scans scans to 52.00° 2 θ . The structure was solved in the space group *Fddd* by direct methods with SHELXTL. The non-hydrogen atoms in the asymmetric unit were modelled with anisotropic displacement parameters. Of the 31 hydrogen atoms included in the model 5 were located and modelled with isotropic displacement parameters, and a riding atom model was used for the remainder.

S9. Host-Guest Interactions

9.1.1 Pillar[n]arenes

The macrocyclic pillar[n]arenes^{20, 21} are proving to exhibit host-guest recognition, including binding of N-alkylated pyridines²² and paraquat.²³ As a prototype for the development of multi-armed molecular shuttles or supramolecular polymer materials, we considered the binding of the N-alkyl groups of complexes [Ru(**3a**)₂](PF₆)₆, [Ru(**3b**)₂](PF₆)₆, [Ru(**4a**)₂](PF₆)₆ and [Ru(**4a**)₂](PF₆)₆ by pillar[n]arenes.

Binding of 3,5-(N-methyl-4-pyridyl)benzene by pillararenes has not been reported, and we initially considered pillar[5]arene to be an ideal size for the weak binding of both N-alkyl pyridine units on one ligand of these complexes. Pillar[6]arene is known to be a much stronger binder, but its bulky size and t-butyl groups would prevent binding the spacer-free complexes [Ru(**3a**)₂](PF₆)₆ and [Ru(**4a**)₂](PF₆)₆.

Firstly we consider the *N*-methyl derivatives, which are known to be only weakly bound guests for pillar[5]arene. Accordingly, in CD₃CN/CDCl₃ mixtures only very weak binding was observed for both [Ru(**3a**)₂](PF₆)₆ and [Ru(**4a**)₂](PF₆)₆, as measured by NMR peak shifts of the *N*-methyl groups (shifted by <0.02 ppm). The use of the long -(CH₂)₁₁CH₃ derivatives [Ru(**3b**)₂](PF₆)₆ and [Ru(**4b**)₂](PF₆)₆ showed only weak binding (*N*-CH₂-¹H NMR peak shift of 0.10 ppm), but allowed the binding to be studied in both more polar (DMSO) and less polar (DCM) solvents. For these complexes it appears the binding of the *N*-alkyl pyridine groups is too weak to be of use for building larger structures.

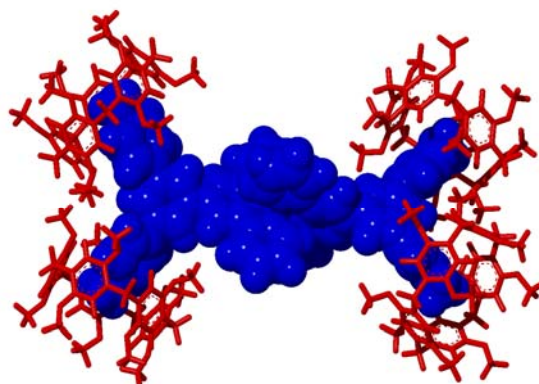
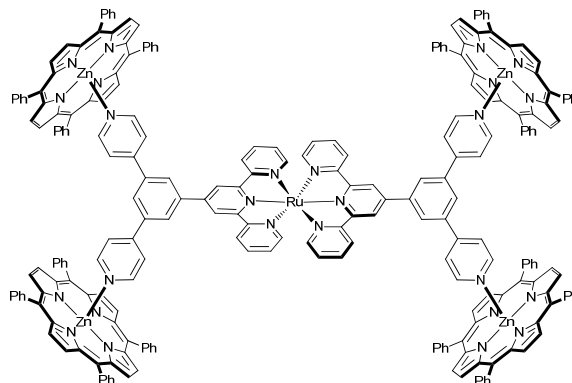


Figure S50 Molecular model (PM3, Spartan) of [Ru(**3a**)₂]⁶⁺ bound by four dimethoxypillar[5]arene molecules.

9.1.2 Metal-ion coordination by [Ru(3a)₂](PF₆)₂

MS sample prepare procedure: Zntpp (2 mg, 0.003 mmol) dissolved in 1ml CHCl₃ was mixed with 0.5 mL MeCN solution of [Ru(1)₂](PF₆)₂ (0.5 mg, 0.0004 mmol). (with a concentration of 0.4mM)



D:\test_1\Zntpp pillar\Zntpp-Ru-suzuki

1/24/2013 10:15:53 AM

Zntpp-Ru-suzuki #12 RT: 0.06 AV: 1 NL: 2.72E3
T: ITMS + p ESI Full ms [120.00-2000.00]

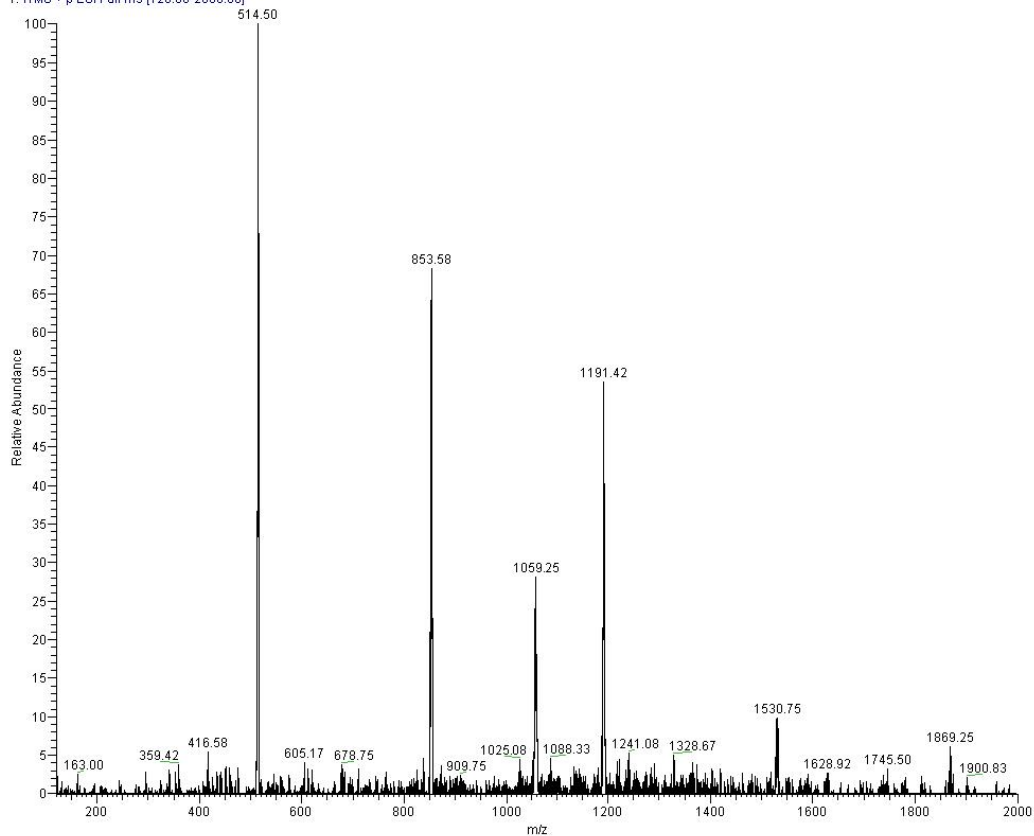


Figure S51 Low-resolution ESI-MS of a mixture of [Ru(1)₂](PF₆)₂ and excess Zntpp. Calculated peaks for $\{[Ru(1)_2]^{2+} + n(Zntpp)\}^{2+}$: 853.2138, 1192.2940, 1531.3743, 1869.9546

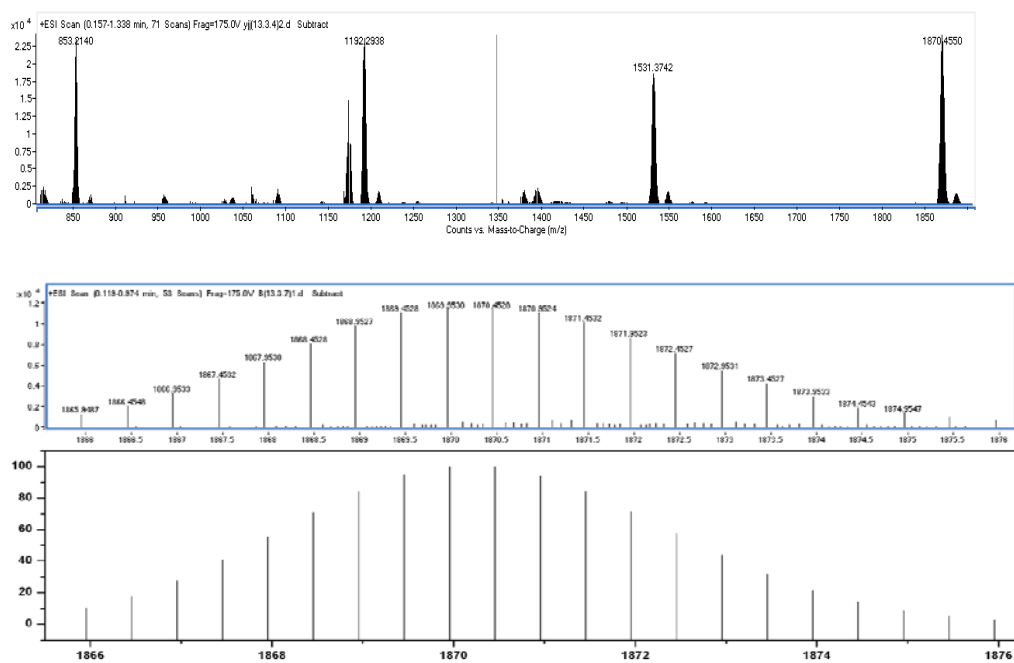
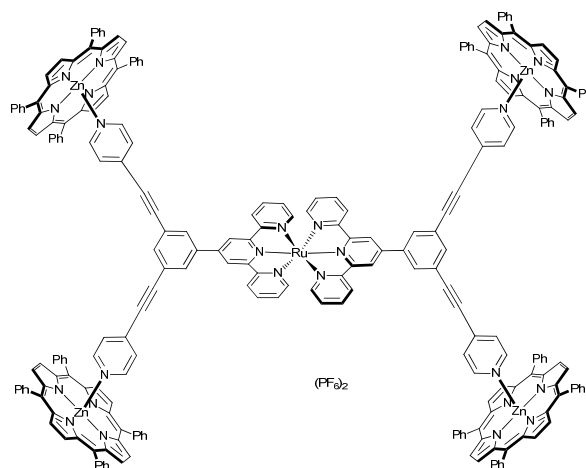


Figure S52 High-resolution ESI-MS of a mixture of $[\text{Ru}(\mathbf{1})_2](\text{PF}_6)_2$ and excess Zntpp. Expansion of peak $\{[\text{Ru}(\mathbf{1})_2]^{2+} + 4(\text{Zntpp})\}^{2+}$ with calculated spectrum shown below.

9.1.3 Metal-ion coordination by [Ru(3b)₂](PF₆)₂

MS sample prepare procedure: Zn₄tp₄ (2mg, 0.003 mmol) dissolved in 1ml CHCl₃ was mixed with 0.5mL MeCN solution of [Ru(2)₂](PF₆)₂ (0.5mg, 0.0004 mmol). (with a concentration of 0.4mM)



D:\test\...Zn₄tp₄-Ru-sonog

1/24/2013 10:17:42 AM

Zn₄tp₄-Ru-sonog #13-15 RT: 0.07-0.07 AV: 3 NL: 1.31E3
T: ITMS + p ESI Full ms [120.00-2000.00]

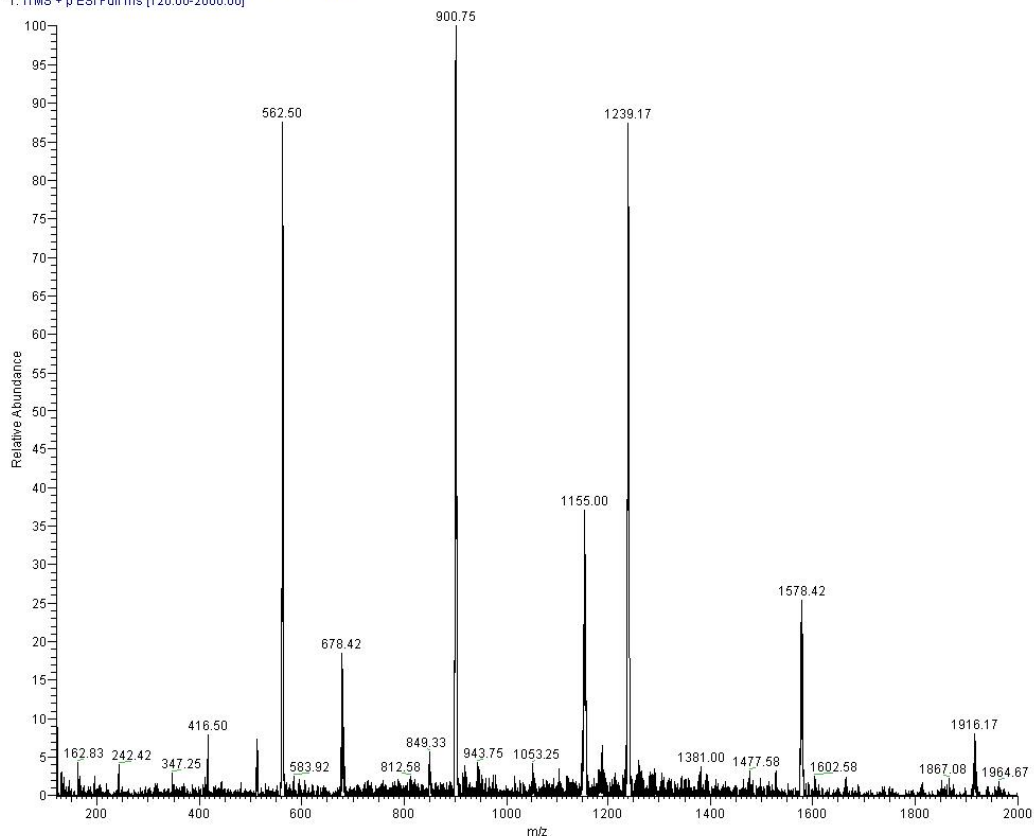


Figure S53 Low-resolution ESI-MS of a mixture of [Ru(2)₂](PF₆)₂ and excess Zn₄tp₄. Calculated peaks for {[Ru(2)₂]²⁺ + n(Zn₄tp₄)²⁺}: 901.2137, 1240.2940, 1579.3743, 1918.4545.

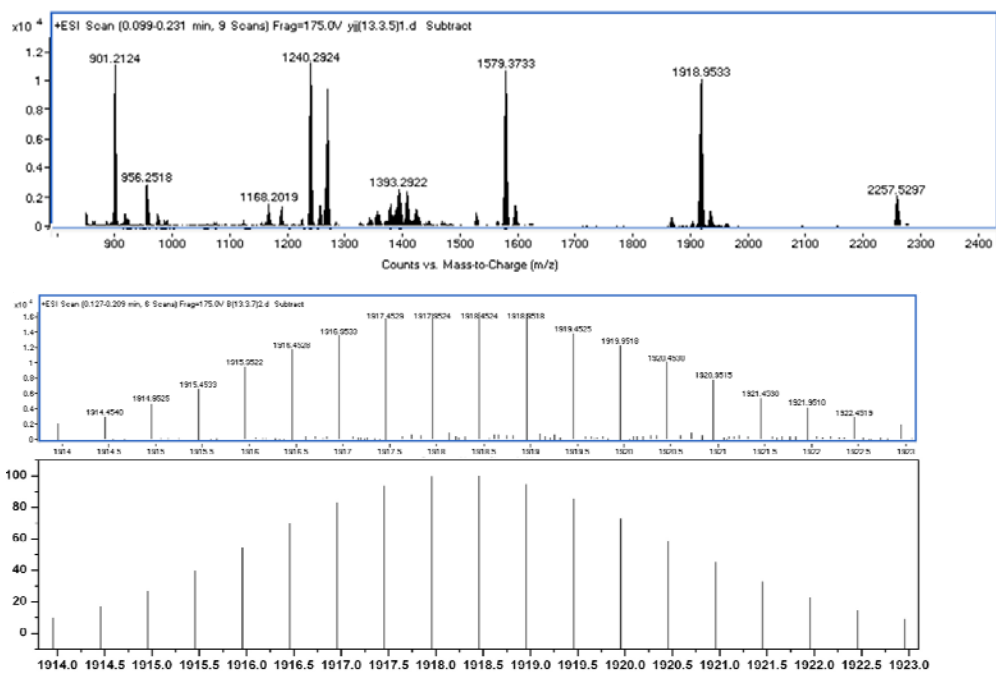


Figure S54 High-resolution ESI-MS of a mixture of $[\text{Ru}(\mathbf{2})_2](\text{PF}_6)_2$ and excess Zntpp. Expansion of peak $\{[\text{Ru}(\mathbf{2})_2]^{2+} + 4(\text{Zntpp})\}^{2+}$ with calculated spectrum shown below.

9.1.4 Association constant determinations

Separate stock solutions of $[\text{Ru}(\mathbf{1})_2](\text{PF}_6)_2$ and $[\text{Ru}(\mathbf{2})_2](\text{PF}_6)_2$ were prepared in 1:2 $\text{CD}_3\text{CN}:\text{CDCl}_3$ (6mL each, 1.14×10^{-4} mol/L for $[\text{Ru}(\mathbf{1})_2](\text{PF}_6)_2$ and 1.30×10^{-4} mol/L for $[\text{Ru}(\mathbf{2})_2](\text{PF}_6)_2$). From these stock solutions, 0.4mL aliquots were used for the NMR titrations.

Zntpp was dissolved in each of the stock solutions to give final concentrations of Zntpp of 1.38×10^{-2} mol/L and 1.47×10^{-2} mol/L in $[\text{Ru}(\mathbf{1})_2](\text{PF}_6)_2$ and $[\text{Ru}(\mathbf{2})_2](\text{PF}_6)_2$ respectively. 10-1000 μL of the Zntpp solutions were added to the Ru(II) aliquots and the NMR peak shifts monitored. The data was fitted using the Matlab program by Thordarson²⁴ using the chemical shifts of 4 NMR peaks.

Table S3 NMR titration data for $[\text{Ru}(\mathbf{1})_2](\text{PF}_6)_2$ with Zntpp ^a

[H] ^b	[G] ^b	Chemical shifts (ppm) ^c			
		H ^{B3}	H ^{A3}	H ^{D3}	H ^{A6}
4.55E-04	0.00E+00	9.135	8.732	7.891	7.415
4.55E-04	6.88E-05	9.106	8.715	7.831	7.377
4.55E-04	1.37E-04	9.083	8.703	7.774	7.362
4.55E-04	2.04E-04	9.064	8.691	7.724	7.349
4.55E-04	2.71E-04	9.034	8.673	7.664	7.336
4.55E-04	3.37E-04	9.002	8.645	7.577	7.315
4.55E-04	5.00E-04	8.952	8.616	7.419	7.284
4.55E-04	6.58E-04	8.906	8.586	7.348	7.262
4.55E-04	8.13E-04	8.865	8.557	7.238	7.238
4.55E-04	9.65E-04	8.834	8.534	7.134	7.214
4.55E-04	1.26E-03	8.785	8.507	7.045	7.189
4.55E-04	1.54E-03	8.753	8.489	6.974	7.177
4.55E-04	1.80E-03	8.732	8.471	6.913	7.156
4.55E-04	2.30E-03	8.648	8.414	6.711	7.11
4.55E-04	2.77E-03	8.575	8.367	6.525	7.069
4.55E-04	3.77E-03	8.500	8.317	6.34	7.022
4.55E-04	4.61E-03	8.461	8.283	6.25	6.996
4.55E-04	5.93E-03	8.435	8.274	6.193	6.979
4.55E-04	7.68E-03	8.426	8.268	6.164	6.972
4.55E-04	8.80E-03	8.42	8.257	6.149	6.969
4.55E-04	9.57E-03	8.416	8.249	6.140	6.967
4.55E-04	9.73E-03	8.411	8.253	6.130	6.963

^a Measured in 1:2 CD₃CN:CDCl₃ at 500 MHz.; ^b [H] = host concentration = 4 × [Ru(**1**)₂]²⁺; [G] = [Zntpp]; ^c Labels refer to proton positions, see Fig 1 in main paper for structure.

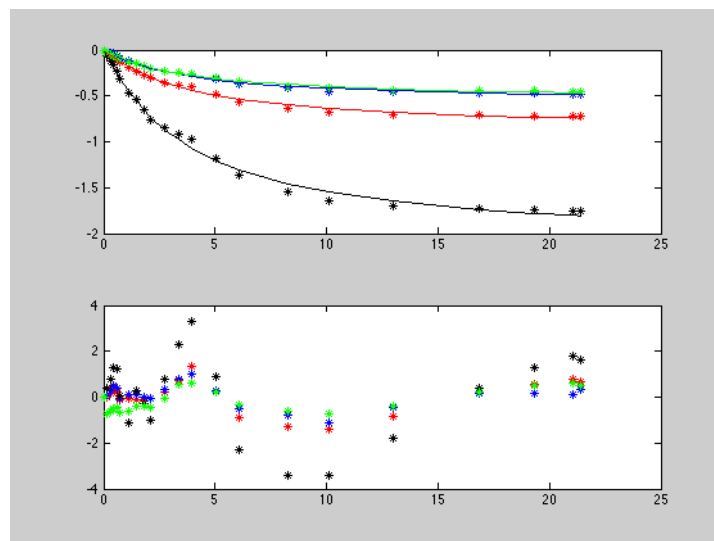


Figure S54 Fitting of NMR titration data in Table S3. Top plot shows (x) equivalents of Zntpp added for each of the four NMR peaks against (y) $\Delta\delta$ (ppm) and the bottom is the residual from the fit.

Table S4 NMR titration data for $[\text{Ru}(\mathbf{2})_2](\text{PF}_6)_2$ with Zntpp ^a

[H] ^b	[G] ^b	Chemical shifts (ppm) ^c			
		H ^{A4}	H ^{D2}	H ^{D3}	H ^{A5}
5.19E-04	0.00E+00	7.964	8.662	7.493	7.229
5.19E-04	7.31E-05	7.959	8.493	7.412	7.217
5.19E-04	1.45E-04	7.947	8.269	7.349	7.21
5.19E-04	2.17E-04	7.932	8.125	7.333	7.199
5.19E-04	2.88E-04	7.93	7.985	7.289	7.196
5.19E-04	3.58E-04	7.922	7.888	7.251	7.198
5.19E-04	5.31E-04	7.917	7.620	7.183	7.183
5.19E-04	6.99E-04	7.909	7.410	7.131	7.181
5.19E-04	8.64E-04	7.891	6.986	6.986	7.155
5.19E-04	1.02E-03	7.875	6.609	6.872	7.139
5.19E-04	1.34E-03	7.856	6.287	6.775	7.122
5.19E-04	1.63E-03	7.83	5.730	6.606	7.096
5.19E-04	2.19E-03	7.825	5.511	6.541	7.091
5.19E-04	2.70E-03	7.817	5.369	6.497	7.083
5.19E-04	3.81E-03	7.728	5.077	6.411	7.07
5.19E-04	4.90E-03	7.727	4.882	6.347	7.06
5.19E-04	6.29E-03	7.729	4.689	6.288	7.054
5.19E-04	8.16E-03	7.728	4.555	6.265	7.047
5.19E-04	9.35E-03	7.729	4.526	6.242	7.045
5.19E-04	1.02E-02	7.728	4.499	6.235	7.042
5.19E-04	1.05E-02	7.729	4.486	6.228	7.044

^a Measured in 1:2 CD₃CN:CDCl₃ at 500 MHz.; ^b [H] = host concentration = 4 × [Ru(2)₂]²⁺; [G] = [Zntpp]; ^c Labels refer to proton positions, see Fig 1 in main paper for structure.

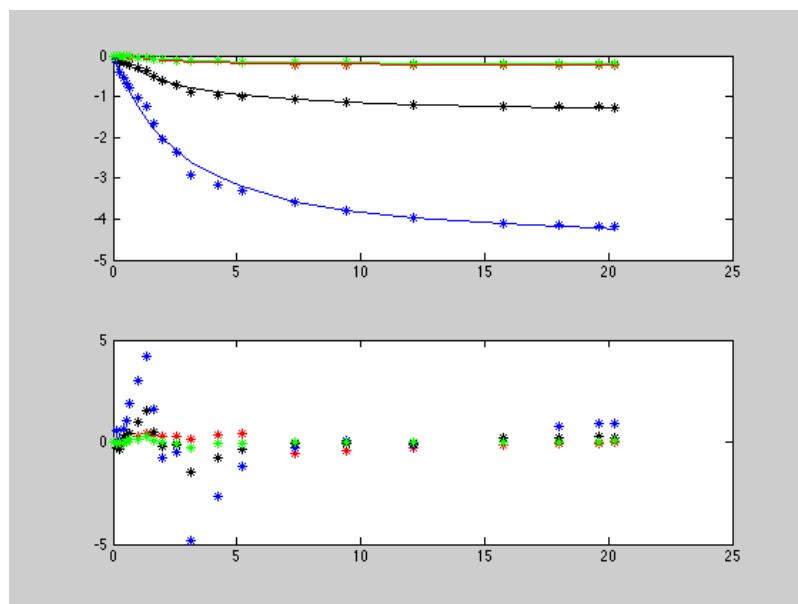


Figure S54 Fitting of NMR titration data in Table S4. Top plot shows (x) equivalents of Zntpp added for each of the four NMR peaks against (y) $\Delta\delta$ (ppm); and the bottom is the residual from the fit..

S10. Additional References

1. J. Wang and G. S. Hanan, *Synlett*, 2005, **2005**, 1251-1254.
2. M. A. Bartucci, P. M. Wierzbicki, C. Gwengo, S. Shajan, S. H. Hussain and J. W. Ciszek, *Tetrahedron Lett.*, 2010, **51**, 6839-6842.
3. C. Coudret, *Synth. Commun.*, 1996, **26**, 3543-3547.
4. I. P. Evans, A. Spencer and G. Wilkinson, *J. Chem. Soc., Dalton Trans.*, 1973, **0**, 204-209.
5. V. Balzani, A. Juris, M. Venturi, S. Campagna and S. Serroni, *Chem. Rev.*, 1996, **96**, 759-834.
6. J. E. Beves, E. C. Constable, C. E. Housecroft, M. Neuburger, S. Schaffner and J. A. Zampese, *Inorg. Chem. Commun.*, 2008, **11**, 1006-1008.
7. E. C. Constable, C. E. Housecroft, M. Neuburger, D. Phillips, P. R. Raithby, E. Schofield, E. Sparr, D. A. Tocher, M. Zehnder and Y. Zimmermann, *J. Chem. Soc., Dalton Trans.*, 2000, 2219-2228.
8. E. C. Constable and A. M. W. C. Thompson, *J. Chem. Soc., Dalton Trans.*, 1994, 1409-1418.
9. M. Maestri, N. Armaroli, V. Balzani, E. C. Constable and A. M. W. C. Thompson, *Inorg. Chem.*, 1995, **34**, 2759-2767.
10. J. E. Beves, E. L. Dunphy, E. C. Constable, C. E. Housecroft, C. J. Kepert, M. Neuburger, D. J. Price and S. Schaffner, *Dalton Trans.*, 2008, 386-396.
11. J. M. Rao, D. J. Macero and M. C. Hughes, *Inorg. Chim. Acta*, 1980, **41**, 221-226.
12. Bruker-Nonius (2003). APEX v2.1, SAINT v.7 and XPREP v.6.14. Bruker AXS Inc. Madison, Wisconsin, USA.
13. WinGX-32: System of programs for solving, refining and analysing single crystal X-ray diffraction data for small molecules, Farrugia, L. J., *J. Appl. Cryst.* 1999, **32**, 837
14. A. Altomare, M. C. Burla, M. Camalli, G. L. Casciarano, C. Giacavazzo, A. Guagliardi, A. G. C. Moliterni, G. Polidori, and S. Spagna, *J. Appl. Cryst.*, 1999, **32**, 115.
15. M. Sheldrick, TWINABS and SADABS: Empirical Absorption and Correction Software, University of Göttingen, Germany, 1999-2003
16. G. M. Sheldrick, SHELXL-97: Programs for Crystal Structure Analysis, University of Göttingen, Germany, 1997
17. P. van der Sluis and A. L. Spek, *Acta Crystallographica Section A*, 1990, **46**, 194-201.
18. A. L. Spek, *PLATON: A Multipurpose Crystallographic Tool*, (2008) Utrecht University, Utrecht, The Netherlands.
19. Bruker-Nonius, *CELL_NOW*, (2003) Bruker AXS Inc., Madison, Wisconsin, USA, Madison Wisconsin, USA.
20. M. Xue, Y. Yang, X. Chi, Z. Zhang and F. Huang, *Acc. Chem. Res.*, 2012, **45**, 1294-1308.
21. P. J. Cragg and K. Sharma, *Chem. Soc. Rev.*, 2012, **41**, 597-607.
22. C. Li, Q. Xu, J. Li, Y. Feina and X. Jia, *Org. Biomol. Chem.*, 2010, **8**, 1568-1576.
23. G. Yu, X. Zhou, Z. Zhang, C. Han, Z. Mao, C. Gao and F. Huang, *J. Am. Chem. Soc.*, 2012, **134**, 19489-19497.
24. P. Thordarson, *Chem. Soc. Rev.*, 2011, **40**, 1305-1323.